

Two-Dimensional Modeling and Analysis of Generalized Random Mobility Models for Wireless Ad Hoc Networks

Denizhan N. Alparslan and Khosrow Sohraby, *Senior Member, IEEE*

Abstract—Most important characteristics of wireless ad hoc networks such as link distance distribution, connectivity, and network capacity are dependent on the long-run properties of the mobility profiles of communicating terminals. Therefore, the analysis of the mobility models proposed for these networks becomes crucial. The contribution of this paper is to provide an analytical framework that is generalized enough to perform the analysis of realistic random movement models over two-dimensional regions. The synthetic scenarios that can be captured include hotspots where mobiles accumulate with higher probability and spend more time, and take into consideration location and displacement dependent speed distributions. By the utilization of the framework to random waypoint mobility model, we derive an approximation to the spatial distribution of terminals over rectangular regions. We validate the accuracy of this approximation via simulation, and by comparing the marginals with proven results for one-dimensional regions we find out that the quality of the approximation is insensitive to the proportion between dimensions of the terrain.

Index Terms—Mobility Modeling, Long-Run Analysis, Ad Hoc Networks, Two-Dimensional Regions.

I. INTRODUCTION

IN WIRELESS ad hoc networks communicating terminals move with respect to many different mobility patterns each one having unique attributes. Therefore, mobility modeling and its analysis become very important for the performance evaluation of these kinds of networks. In this paper, we focus on the long-run location and speed distribution analysis of a generalized random mobility modeling approach over two-dimensional mobility terrains.

The modeling methodology we are concentrating on is originally defined in [1] as a generalized model that is flexible enough to capture the major characteristics of several realistic movement profiles. In that paper, long-run location and speed distributions are given in closed form expressions for one-dimensional regions. Here, we extend the analysis to two-dimensional terrains. A variety of examples are also given to show how the proposed model and its long-run analysis framework work for a broad range of mobility modeling approaches.

In what follows, we give a brief description of the generalized random mobility characterization approach that is analyzed in this article. Let R denote the two-dimensional

bounded region on which mobile terminals operate. A mobile located at the point $X_s = (X_{s_1}, X_{s_2}) \in R$, selects a random point $X_d = (X_{d_1}, X_{d_2}) \in R$ as destination according to the conditional probability density function (pdf) $f_{X_d|X_s}(x_d|x_s)$, and moves to point X_d on the straight line segment joining the two points, and at a speed V that is drawn randomly from the interval $[v_{\min}, v_{\max}]$, where $v_{\min} > 0$, according to the conditional pdf $f_{V|X_s, X_d}$. After reaching the destination, mobile pauses for a random amount of time, denoted by T_p , at X_d , which is distributed with respect to the conditional pdf $f_{T_p|X_d}$, and whole cycle is repeated by selecting a new destination. Hence, the pattern of a mobile terminal is composed of consecutive movement epochs between the randomly selected points X_s and X_d , and it is uncorrelated with the movement behaviors of other terminals. Throughout this paper, we use the triplet $\langle f_{X_d|X_s}, f_{V|X_s, X_d}, f_{T_p|X_d} \rangle$ to characterize the movement pattern of a mobile that moves with respect to this model.

Among the parameters of the triplet $\langle f_{X_d|X_s}, f_{V|X_s, X_d}, f_{T_p|X_d} \rangle$, the conditional pdf $f_{X_d|X_s}$ identifies the distribution of X_d given X_s at the embedded points in time where a new movement epoch starts. Incorporation of this kernel into this mobility characterization methodology provides the ability to define hotspots on the two-dimensional mobility terrain where mobiles accumulate with higher probability, and correlations between consecutive hotspot decisions can be successfully modeled. Furthermore, since V is randomly drawn from $f_{V|X_s, X_d}$, we have the flexibility of constructing a correlation between the distribution of V and the locations of the starting point X_s and destination X_d . For instance, a scenario that identifies V proportional to the distance that is going to be traveled, that is, $|X_s - X_d|$, can be easily defined. In addition, the usage of $f_{T_p|X_d}$ makes it possible to capture different pause distributions at different destinations available for the mobility model.

For wireless ad hoc networks, there have been proposed a number of different mobility models. Comprehensive surveys of these models can be found in [2], [3]. Among them, the random waypoint model [4] is one of the most widely used one for analytic and simulation-based performance analysis of ad hoc networks. In this model, a mobile selects a destination point in the mobility terrain with equal probability, and moves to that point with a speed that is drawn uniformly from a given range. After reaching the destination, mobile pauses for a random time, which has a distribution that is independent from the current location, and whole cycle is repeated by selecting a new destination. In [5], [6], [7], analytical frameworks are presented for the long-run analysis of this mobility model.

(c)20xx IEEE. Personal use of this material is permitted. However, permission to reprint/republish this material for advertising or promotional purposes or for creating new collective works for resale or redistribution to servers or lists, or to reuse any copyrighted component of this work in other works, must be obtained from the IEEE.

D. N. Alparslan is with The MathWorks, Inc., MA, USA

K. Sohraby is with School of Computing and Engineering, University of Missouri - Kansas City, MO, USA

The analysis that we propose in this paper is also applicable to random waypoint model, and to demonstrate the correctness and superiority of our work, we present a comparison of the results derived with the ones presented in literature.

The rest of this paper is outlined as follows. In Section II, we describe analytical framework we developed for long-run analysis. Section III provides the long-run distributions for a limited version of the exact mobility formulation constructed according to the methodology explained in the second section. Section IV utilizes the results reached in section three to derive approximations for the long-run distributions of the generalized model proposed. In Section V, we focus on example scenarios, and the final section presents a summary of the paper.

II. METHODOLOGY AND DESCRIPTION OF ANALYTICAL FRAMEWORK

In this section, we describe the analytical framework we establish for the long-run analysis of the generalized mobility model proposed.

Now since the movement behavior of mobiles are assumed to be uncorrelated with each other, we can concentrate on a single terminal for long-run analysis. Hence, for the terminal whose movement pattern is characterized by the triplet $\langle f_{X_d|X_s}, f_{V|X_s, X_d}, f_{T_p|X_d} \rangle$, let the vector $\mathbf{X}(t)$ denote the state descriptor whose components identify the current location, destination, and the speed of that mobile at time t . In our solution methodology, we discretize the two-dimensional mobility terrain R and approximate the random variable V with a discrete random variable so that the stochastic process $\{\mathbf{X}(t), t \geq 0\}$ can be defined on a multidimensional discrete state space. The assumptions that we have made to generate this discrete state space are as follows:

A_1 : The bounded region R is discretized into n disjoint, non-overlapping cells of the same shape denoted by c_i , $i = 0 \dots n - 1$, such that $R \subseteq \bigcup_{i=0}^{n-1} c_i$ where $n > 1$. A mobile terminal is assumed to occupy one of the c_i 's at any moment in time, and movement epochs occur between two randomly picked starting and destination cells.

A_2 : The random variable V , that is, the speed during a movement epoch, is approximated by the discrete random variable V^* defined on the state space $\mathcal{S}_{V^*} = \{z_1, z_2, \dots, z_m\}$ where $z_r = r \Delta v$, $r = 1, \dots, m$, for some discretization parameter $\Delta v > 0$, and an integer $m \geq 1$ such that $\Delta v \leq v_{\min}$ and $v_{\max} = m \Delta v$.

Based on these assumptions, observe that a mobile can be in pausing or moving modes at the cell it is currently located.

Additionally, instead of observing the state of a terminal continuously, we observe it at embedded times denoted by T_k , for $k \in \mathbf{N}$, such that $T_0 = 0$, $T_{k+1} \geq T_k$, $\forall k \in \mathbf{Z}^+$, which point to the time of occurrence of one of the following events:

E_1 : The terminal which is in pause mode, selects a new cell as destination that is different from the current cell occupied, and changes its state to moving state in the current cell it is located,

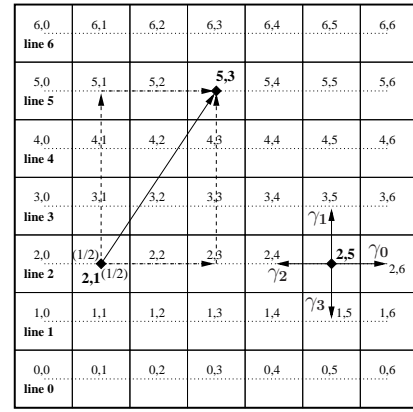


Fig. 1. Discretization of the square region R into squares.

E_2 : The terminal which is traveling in the direction of the target cell, moves out from the current cell and enters the neighboring cell that lies on the shortest path between the current and destination cells,

E_3 : The terminal reaches to the destination cell and enters the pause mode at that location.

In our analysis, to apply assumption A_1 , which is done to approximate the exact location that can be occupied by a terminal at any point in time, we focus on the discretization methods that partition the region R into squares or hexagons. The reasoning behind concentrating on two different discretization approaches for R concurrently will become more clear as we proceed further in the long-run analysis. In Fig. 1, we apply the square discretization approach to a square region. Visualization of a discretization that is performed by hexagons can be found in [8].

In Fig. 1, we also depict the scheme we decide on to identify the cells on the discretized region. Basically, the centers of the cells are grouped by lines that are parallel to each other, and the index i of cell c_i is denoted by $i = (\ell_i, \ell'_i)$ where ℓ_i represents the line that the center of c_i is located, and ℓ'_i is its location on that line. For the rest of this paper, we will use the notations c_i and $c_{(\ell_i, \ell'_i)}$ interchangeably. Hence, if there are n_ℓ lines, and if q_ℓ denotes the number of cells on line ℓ , then set of the cells on the discretized region can be defined as follows:

$$\tilde{R} = \bigcup_{\ell=0}^{n_\ell-1} \{c_{(\ell,0)}, \dots, c_{(\ell,q_\ell-1)}\}, \quad (1)$$

Clearly, the path traveled during a movement epoch described by the discretized version of the mobility characterization we constructed is composed of consecutive straight line segments between the centers of the cells c_i , $i = 0, \dots, n - 1$. In other words, a mobile terminal moves to one of the neighboring cells from the current cell occupied while traveling towards the destination cell. Hence, if d denotes the number of available movement directions for the discretized mobility formulation, then d would be equal to the number of the sides of the regular polygons used in the discretization process. Thus, $d = 4$ for square discretization, and $d = 6$ for hexagonal discretization, and let $\gamma_{i,\ell} = 0, \dots, d - 1$ denote those directions (see cell $c_{(2,5)}$ in Fig. 1). On the other hand, in principle, if there are no obstacles on the region R that can restrict the movement directions, then mobile should be able to move at any direction. Therefore, by discretizing the region,

we are also forced to *discretize the movement direction*. Obviously, if R is discretized by regular polygons of the same shape, as we are doing, then d can be at most equal to six. Furthermore, if the discretization of a region R with a general shape (e.g. rectangle) with regular polygons is done for the purpose approximating the exact location of a terminal, as in our case, then using hexagons is a better choice because the number of available movement directions are higher, and a more realistic approximation can be done to the exact mobility pattern.

At this point, it should be noted that, the enforcement of discretizing movement directions will not arise for the one-dimensional case because there are only two directions for a mobile to move on a one-dimensional region and discretization method does not enforce any kind of restriction on these directions. Clearly the fundamental difference between the discretization parameters d , and n and m is that n and m can be increased, but d , as we have mentioned above, can be at most equal to six. This difference introduces a new issue that has to be clarified before continuing. In what follows, we explain this issue and our solution approach for it.

Now recall that according to our mobility model proposed, during a movement epoch, mobile travels on the straight line joining the points X_s and X_d . In the discretized version of this mobility model, movement epochs occur between randomly selected cells. Obviously if the mobile terminal is allowed to move at any direction in the region R , then the shortest path between those two points is just the straight line between them, and it is unique. However, for the discrete formulation, the shortest path is defined in terms of the number of jumps between cells. More importantly, for a discretization that is done according to squares (i.e., $d = 4$), or to hexagons (i.e., $d = 6$), if $\tilde{p}^{(d)}(i, j)$, $d = 4, 6$, denotes the ordered list of the cells that are located on a shortest path for the movement epoch that had started at c_i , and ended up at destination cell c_j , then the members of $\tilde{p}^{(d)}(i, j)$ will not be necessarily unique. The algorithm that we use in this paper to generate $\tilde{p}^{(d)}(i, j)$ is as follows. If c_j is towards the direction $\gamma_{i'}$ for some $i' \in \{0, \dots, d-1\}$ from c_i , then mobile follows that direction until it reaches destination c_j . On the other hand, mobile proceeds to the next cell either in the direction $\gamma_{i'}$ or $\gamma_{i'+1 \bmod d}$ with equal probabilities for some $i' \in \{0, \dots, d-1\}$ that generates the least possible shortest path if selected, and continues in that direction until it reaches to a cell that can be joined to c_j by following one of the d available directions. For example, in Fig. 1, consider the scenario where $c_i = c_{(2,1)}$ and $c_j = c_{(5,3)}$. Observe that for this scenario, this algorithm either generates the path $\{c_{(2,1)}, c_{(2,2)}, c_{(2,3)}, c_{(3,3)}, c_{(4,3)}, c_{(5,3)}\}$ or the path $\{c_{(2,1)}, c_{(3,1)}, c_{(4,1)}, c_{(5,1)}, c_{(5,2)}, c_{(5,3)}\}$. It should be also noted that, according to our notation, the first and the last members of the list $\tilde{p}^{(d)}(i, j)$ are c_i and c_j , respectively.

Having clarified these issues, we now proceed to the formal definition of the discretized mobility formulation. Denote \mathbf{S}_k , $k \in \mathbf{N}$, as the state of the mobile terminal at time T_k . Hence, based on assumptions A_1 , A_2 , and the events E_1 , E_2 , E_3 that identify observation times T_k , for $k \in \mathbf{N}$, the finite state-space of \mathbf{S}_k will be defined as follows:

$$\mathcal{S} = \mathcal{S}_{\mathcal{M}} \cup \mathcal{S}_{\mathcal{P}} \quad (2)$$

where

$$\mathcal{S}_{\mathcal{M}} = \{(c_i, c_j, z_r, q) \mid i, j = 0, \dots, n-1, i \neq j, \\ r = 1, \dots, m, q = 1\} \quad (3)$$

$$\mathcal{S}_{\mathcal{P}} = \{(c_i, q) \mid i = 0, \dots, n-1, q = 0\} \quad (4)$$

where c_i is the current cell occupied, c_j is the destination cell, z_r is the discretized speed, and q is the indicator function that is defined as follows:

$$q = \begin{cases} 1, & \text{mobile is moving towards the target cell} \\ 0, & \text{mobile is pausing at the destination cell} \end{cases} \quad (5)$$

Consequently, the stochastic process $\{\mathbf{X}(t), t \geq 0\}$ can be formally defined on the finite-state space \mathcal{S} according to the following expression:

$$\mathbf{X}(t) = \mathbf{S}_k, \quad \text{if } T_k \leq t < T_{k+1}$$

Notice that when $\mathbf{X}(t)$ occupies a state $s \in \mathcal{S}_{\mathcal{M}}$, since the state s has a separate dimension for the destination cell, the next state to be visited can be determined from the components of it. In other words, the future evolution of the stochastic process $\{\mathbf{S}_k, k \in \mathbf{N}\}$ becomes dependent only on the current state of the mobile terminal, not on its history at previous observation points. Furthermore, for all $s \in \mathcal{S}$, the distribution of sojourn time in state s would be independent from the previous states occupied and can be determined only from the components of state s .

Therefore, the stochastic process $\{\mathbf{S}_k, T_k; k \in \mathbf{N}\}$ with finite-state space \mathcal{S} satisfies the conditions for being *Markov Renewal Process*, and the process $\{\mathbf{X}(t), t \geq 0\}$ can be called as the *semi-Markov process* (SMP) associated with $\{\mathbf{S}_k, T_k; k \in \mathbf{N}\}$ [9]. Moreover, since the distributions for destination, speed, and pause time parameters are assumed to be *time-homogeneous* in the mobility model proposed, the distribution of state holding time in state s , given that the next state to be visited is s' , would be independent of k . Hence, the transitions of the process $\mathbf{X}(t)$ at the embedded time instants T_k can be governed by the *discrete-time* Markov chain (DTMC) $\{\mathbf{S}_k, k \in \mathbf{N}\}$ with finite-state space \mathcal{S} in (2) and transition probability matrix $P = [p_{ss'}]$, where $p_{ss'} = \Pr\{\mathbf{S}_{k+1} = s' \mid \mathbf{S}_k = s\}$, such that $\sum_{s' \in \mathcal{S}} p_{ss'} = 1$ for all $s \in \mathcal{S}$. The process $\{\mathbf{S}_k, k \in \mathbf{N}\}$ is also referred as *embedded DTMC* of SMP.

Thus, in order to characterize the SMP $\{\mathbf{X}(t), t \geq 0\}$ at the long-run, the DTMC $\{\mathbf{S}_k, k \in \mathbf{N}\}$ must satisfy the ergodicity conditions and the mean state holding times must be finite. If these conditions are satisfied, then the long-run proportion of time spent in a state $s \in \mathcal{S}$ can be obtained, and after aggregating the states that has the same *current cell* and *speed* components, the long-run distributions sought can be derived for this discretized version of the mobility formulation.

Notice that, as the discretization parameters $n \rightarrow \infty$ and $m \rightarrow \infty$, we obtain better approximations to the location and speed of the mobile terminals, respectively, and in the limit we converge to a restricted version the continuous model where the available movement directions are limited by the d different directions $\gamma_0, \dots, \gamma_{d-1}$ given by

$$\gamma_i = \begin{cases} \frac{2\pi i}{d}, & \text{if } d = 4, \\ \frac{2\pi(i+1/2)}{d}, & \text{if } d = 6, \end{cases} \quad (6)$$

for $i = 0, \dots, d-1$. Visualization of these directions are also provided in Fig. 1 for $d = 4$. Clearly because of the methodology we decided to generate $\tilde{p}^{(d)}(i, j)$, at the limit $n \rightarrow \infty$, the path followed during a movement epoch between X_s and $X_d \in R$ will generally be composed of two directed finite line segments towards the directions γ_{i_1} and γ_{i_2} where $\{i_1 = i, i_2 = (i+1) \bmod d\}$ or $\{i_1 = (i+1) \bmod d, i_2 = i\}$ for some $i \in \{0, \dots, d-1\}$. This can be also observed from the example movement scenarios depicted in Fig. 1. Obviously if X_d is towards any of directions γ_i , $i = 0, \dots, d-1$, from X_s , then the path will be composed of a single straight line. For the rest of this report we will use the term *continuous-d mobility formulation* to refer to this limited version of the exact continuous mobility formulation. Finally, we note that, since d can be at most equal to six, a formal transition from this limited case to the original continuous formulation cannot be done. Therefore, in the following sections we will use distributions of the continuous- d mobility formulation to gain some insight into the methodology that can be used to derive approximations for the long-run distributions of original case.

III. ANALYTICAL RESULTS FOR THE DISCRETIZED AND CONTINUOUS- d MOBILITY FORMULATION

In this section, we first concentrate on generating the long-run location and speed distributions for the discretized case, and after that we will use those results to derive long-run distributions of the continuous- d mobility formulation.

Now, to able to identify the transition probabilities of the DTMC $\{\mathbf{S}_k, k \in \mathbf{N}\}$, we first denote $\tau_{j|i}$ as the probability of selecting cell c_j as target from cell c_i . Then, according to the mobility characterization parameter $f_{X_d|X_s}$, $\tau_{j|i}$ will be given by

$$\tau_{j|i} = \int_{x_d \in c_j} f_{X_d|X_s}(x_d|X_s \in c_i) dx_d, \quad (7)$$

Similarly, denote $\nu_{r|i,j}$ as the conditional probability mass function of V^* for a movement epoch that had started at cell c_i with destination c_j . Then, by using the parameter $f_{V|X_s, X_d}$ we have

$$\nu_{r|i,j} = \int_{(r-1)\Delta v}^{r\Delta v} f_{V|X_s, X_d}(v|X_s \in c_i, X_d \in c_j) dv \quad (8)$$

for $r = 1, \dots, m$. In addition, let $n_h(c_i)$ denote the cells in the neighborhood of cell c_i that can be reached in one jump from it, and let $[i', i, j]$ denote the index of the cell $c_{i'}$ in the ordered list that defines the path $\tilde{p}^{(d)}(i, j)$. Note that, $[i, i, j] = 1$, and $[j, i, j] = \|\tilde{p}^{(d)}(i, j)\|$ where $\|\tilde{p}^{(d)}(i, j)\|$ denotes the number of the cells on the path $\tilde{p}^{(d)}(i, j)$. Hence, if we are interested in the probability of the cell $c_{i'}$ to be the next cell to be visited after cell c_i , that is, $\Pr\{[i', i, j] = 2\}$, then $\Pr\{[i', i, j] = 2\}$ is either equal to 1, or 1/2, or 0 (i.e. $c_{i'}$ is not on the path $\tilde{p}^{(d)}(i, j)$). For instance, in Fig. 1, when $c_i = c_{(2,1)}$, $c_j = c_{(5,3)}$, and $c_{i'} = c_{(2,2)}$, then $\Pr\{[i', i, j] = 2\} = 1/2$. On the other hand, if $c_i = c_{(2,1)}$, $c_j = c_{(2,3)}$, and $c_{i'} = c_{(2,2)}$, then $\Pr\{[i', i, j] = 2\} = 1$.

Based on these definitions, the transition probabilities corresponding to the events E_1 , E_2 , and E_3 , can be grouped as in Table I.

Next, we examine the irreducibility and aperiodicity of the DTMC $\{\mathbf{S}_k, k \in \mathbf{N}\}$ with respect to the transition probabilities defined in Table I. Let φ_i denote the probability of starting a

TABLE I
TRANSITION PROBABILITIES OF THE PROCESS $\{\mathbf{S}_k, k \in \mathbf{N}\}$

Event	Transition	Probability	Condition*
E_1	$(c_i, 0) \rightarrow (c_i, c_j, z_r, 1)$	$\frac{\tau_{j i}}{1 - \tau_{i i}} \nu_{r i,j}$	$i \neq j$
E_2	$(c_i, c_j, z_r, 1) \rightarrow (c_{i'}, c_j, z_r, 1)$	1	$c_j \notin n_h(c_i)$, $\Pr\{[i', i, j] = 2\} = 1$
		1/2	$c_j \notin n_h(c_i)$, $\Pr\{[i', i, j] = 2\} = 1/2$
E_3	$(c_i, c_j, z_r, 1) \rightarrow (c_j, 0)$	1	$c_j \in n_h(c_i)$

* $i, i', j = 0, \dots, n-1$, $r = 1 \dots m$

movement epoch from a cell c_i , $i = 0, \dots, n-1$ at the steady-state. Obviously, in order to satisfy the irreducibility, φ_i must be greater than 0 for all $i = 0, \dots, n-1$. Otherwise, some cells on the two-dimensional discretized region will never be visited (i.e., selected as destination) and the chain becomes reducible. Hence, a steady-state distribution must exist for X_s . The conditional pdf $f_{X_d|X_s}(x_d|x_s)$, which identifies the distribution of X_d given X_s at the embedded points in time where a new epoch starts, is referred as *stochastic density kernel* by Feller [10]. Under some ‘‘mild’’ regularity conditions defined in [10] on $f_{X_d|X_s}(x_d|x_s)$ the steady-state distribution of X_s with pdf $f_{X_s}(x_d)$ can be uniquely determined from the solution of the following integral equation

$$f_{X_s}(x_d) = \int_{x_s \in R} f_{X_d|X_s}(x_d|x_s) f_{X_s}(x_s) dx_s, \quad (9)$$

and φ_i will then be equal to

$$\varphi_i = \int_{x_d \in c_i} f_{X_s}(x_d) dx_d \quad (10)$$

Observe that, if $T = [\tau_{j|i}]$, and if the integral equation (9) has a unique solution, then φ_i can be also obtained by solving $\varphi T = \varphi$, $\|\varphi\|_1 = 1$ where $\varphi = [\varphi_0, \dots, \varphi_{n-1}]$.

In view of the discussions above, the following can be easily proven.

Lemma 1: If the pdf $f_{X_s}(x_d)$ can be uniquely determined from the solution of the integral equation (9), and if $\nu_{r|i,j} > 0$, $i, j = 0, \dots, n-1$ and $r = 1, \dots, m$, then the embedded DTMC $\{\mathbf{S}_k, k \in \mathbf{N}\}$ defined on state space \mathcal{S} in (2), with transition probabilities given as in Table I, is irreducible and aperiodic.

Next, we provide the steady-state distribution of the DTMC $\{\mathbf{S}_k, k \in \mathbf{N}\}$.

Lemma 2: For the DTMC $\{\mathbf{S}_k, k \in \mathbf{N}\}$ defined on the state space \mathcal{S} in (2), where d is either equal four or six, let $\pi_i^{(d)}$ and $\pi_{(i,j,r)}^{(d)}$ denote the steady-state probabilities of being in the states of the form $s = (c_i, 0)$, $i = 0, \dots, n-1$, and $s = (c_i, c_j, z_r, 1)$, $i, j = 0, \dots, n-1$, $i \neq j, r = 1, \dots, m$, respectively. If the conditions of Lemma 1 are satisfied, then they are uniquely given by

$$\pi_i^{(d)} = \varphi_i (1 - \tau_{i|i}) / N, \quad (11)$$

$$\begin{aligned} \pi_{i,j}^{(d)} &= \sum_{c_{i'} \in p_{i,j}^{(d)}} \varphi_{i'} \tau_{j|i'} \nu_{m|i',j} / N \\ &+ \frac{1}{2} \sum_{c_{i'} \in p_{i,2}^{(d)}(i,j)} \varphi_{i'} \tau_{j|i'} \nu_{m|i',j} / N \end{aligned} \quad (12)$$

where

$$\boldsymbol{\pi}_{i,j}^{(d)} = [\pi_{(i,j,1)}^{(d)}, \dots, \pi_{(i,j,m)}^{(d)}], \quad (13)$$

$$\boldsymbol{\nu}_{m|i',j} = [\nu_{1|i',j}, \dots, \nu_{m|i',j}], \quad (14)$$

and

$$p_{i,1}^{(d)}(i,j) = \{c_{i'}|c_{i'} \in \tilde{R}, \Pr\{c_i \in \tilde{p}^{(d)}(i',j)\} = 1\}, \quad (15)$$

$$p_{i,2}^{(d)}(i,j) = \{c_{i'}|c_{i'} \in \tilde{R}, \Pr\{c_i \in \tilde{p}^{(d)}(i',j)\} = 1/2\}, \quad (16)$$

$$\text{and } N = \sum_{i=0}^{n-1} \pi_i^{(d)} + \sum_{i=0}^{n-1} \sum_{\substack{j=0 \\ j \neq i}}^{n-1} \|\boldsymbol{\pi}_{i,j}^{(d)}\|_1.$$

Proof: Refer to [8]. ■

It should be noted that, the sets $p_{i,1}^{(d)}(i,j)$ in (15) and $p_{i,2}^{(d)}(i,j)$ in (16) represent the subset of cells in \tilde{R} from where a movement epoch originated with destination cell c_j passes through the cell c_i with probabilities 1 and 1/2, respectively.

Now, let \bar{t}_s denote the sojourn time of the SMP $\{\mathbf{X}(t), t \geq 0\}$ in state $s \in \mathcal{S}$. Then, if $s = (c_i, c_j, z_r, 1)$ (i.e., mobile is moving towards the destination with discrete speed z_r), and if $\Delta c^{(d)}$ denotes the traveled distance in a cell while passing trough it, then

$$\bar{t}_s = \frac{\Delta c^{(d)}}{z_r} \quad (17)$$

On the other hand, if $s = (c_i, 0)$, then we define the following.

$$\bar{t}_s = E[T_{p_i}] = E[T_p|X_s \in c_i] \quad (18)$$

Finally, in order to characterize the SMP $\{\mathbf{X}(t), t \geq 0\}$ at the long-run, the following must be satisfied [9]:

$$\sum_{s \in \mathcal{S}} \pi_s \bar{t}_s < \infty \quad (19)$$

Hence, by applying the theory of semi-Markov processes we obtained the long-run proportion of time that the SMP $\{\mathbf{X}(t), t \geq 0\}$ is in a state $s \in \mathcal{S}$. After aggregating the states in \mathcal{S} that has the same *current location* and *speed* components, including the ones with zero speed (i.e., $s = (c_i, 0)$), we reach to the following result.

Lemma 3: For the mobile terminal, whose mobility pattern is characterized according to the discretized version of the $\langle f_{X_d|X_s}, f_{V|X_s, X_d}, f_{T_p|X_d} \rangle$ mobility formulation, let $p_i^{(d)}$, $i = 0, \dots, n-1$, $d = 4, 6$, denote the long-run proportion of time that terminal stays in cell c_i , which can be a square or hexagon. Similarly, denote $\psi_r^{(d)}$ as the long-run proportion of time that mobile possesses speed $z_r = r\delta v$, $r = 0, \dots, m$. If the conditions given by Lemma 1 are satisfied, and equation (19) holds to be true, then

$$p_i^{(d)} = \frac{\varphi_i (1 - \tau_{i|i}) E[T_{p_i}] + \sum_{r=1}^m k_{i,r}^{(d)}}{N_{n,m}^{(d)}}, \quad (20)$$

and

$$\psi_r^{(d)} = \begin{cases} \sum_{i=0}^{n-1} \varphi_i (1 - \tau_{i|i}) E[T_{p_i}] / N_{n,m}^{(d)}, & \text{if } r = 0 \\ \sum_{i=0}^{n-1} k_{i,r}^{(d)} / N_{n,m}^{(d)}, & \text{else} \end{cases} \quad (21)$$

where

$$k_{i,r}^{(d)} = \sum_{c_j \in \tilde{R} - \{c_i\}} \left(\sum_{c_{i'} \in p_{i,1}^{(d)}(i,j)} \varphi_{i'} \tau_{j|i'} \frac{1}{z_r} \nu_{r|i',j} \Delta c^{(d)} \right) + \frac{1}{2} \sum_{c_{i'} \in p_{i,2}^{(d)}(i,j)} \varphi_{i'} \tau_{j|i'} \frac{1}{z_r} \nu_{r|i',j} \Delta c^{(d)}, \quad (22)$$

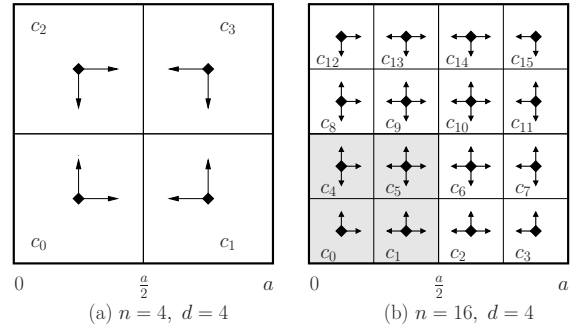


Fig. 2. Discretized version of a simple mobility scenario.

and

$$N_{n,m}^{(d)} = \sum_{i=0}^{n-1} \varphi_i (1 - \tau_{i|i}) E[T_{p_i}] + \hat{D}_n^{(d)} \quad (23)$$

where

$$\hat{D}_n^{(d)} = \sum_{i=0}^{n-1} \sum_{r=1}^m k_{i,r}^{(d)} \quad (24)$$

To simplify the formulation of $\hat{D}_n^{(d)}$ in (24) for some special cases, we now state the following claim.

Claim 1: If the distribution of V^* is assumed to be independent from the location of the starting and destination cells of the movement epochs, the expression for $\hat{D}_n^{(d)}$ in (24) is equivalent to the following:

$$\hat{D}_n^{(d)} = E\left[\frac{1}{V^*}\right] \sum_{c_i \in \tilde{R}} \sum_{c_j \in \tilde{R}} \varphi_i \tau_{j|i} \text{dis}^{(d)}(i,j) \Delta c^{(d)}, \quad (25)$$

where $\text{dis}^{(d)}(i,j) = \|\tilde{p}^{(d)}(i,j)\| - 1$, that is, the number of the discrete jumps made on the path $\tilde{p}^{(d)}(i,j)$.

Proof: Refer to [8]. ■

Before continuing on with the long-run analysis of the continuous- d mobility formulation, in order to clarify the interpretation of term $k_{i,r}^{(d)}$ given in (22), we now concentrate on a simple example scenario. Now, consider a continuous mobility formulation (i.e., mobiles can move anywhere at any direction) over the region $R = [0, a] \times [0, a]$ where V is deterministic and equal v , and the other mobility characterization parameters, $f_{X_d|X_s}$ and $f_{T_p|X_d}$, can be arbitrary as long as the integral equation in (9) is uniquely solvable and equation (19) is satisfied. Now to be able to apply Lemma 3, we need to generate the discretized version of this mobility formulation. Hence, assume $n = 4$, $d = 4$, and since V is deterministic, $m = 1$. In Fig. 2.(a) we provided a visualization of the discretized mobility model generated according to these assumptions.

Now for this discretized mobility formulation, if we are interested in the long-run proportion of time mobile stays in cell c_0 (i.e., $p_0^{(4)}$), then according to Lemma 3 we simply have

$$p_0^{(4)} = \frac{\varphi_0 (1 - \tau_{0|0}) E[T_{p_0}] + k_{0,1}^{(4)}}{N_{4,1}^{(4)}}, \quad (26)$$

where

$$k_{0,1}^{(4)} = \frac{a}{2v} (\varphi_0 \tau_{1|0} + \frac{1}{2} \varphi_2 \tau_{1|2} + \varphi_0 \tau_{2|0} + \frac{1}{2} \varphi_1 \tau_{2|1} + \varphi_0 \tau_{3|0} + \varphi_1 \tau_{0|1} + \varphi_2 \tau_{0|2} + \varphi_3 \tau_{0|3}), \quad (27)$$

which is equal to the average time spent over the cell c_0 while moving between randomly picked cells. In other words, $k_{0,1}^{(4)}$ is equal to $\frac{a/2}{v}$ multiplied with the probability of a movement

epoch between two randomly picked cells that pass through the cell c_0 , including the ones starting or ending at cell c_0 . Notice that in this simple formulation $\nu_{r|i',j} = 1$ for all $i', j = 0, \dots, 3$. However, if the distribution of V is dependent on X_s and X_d in the original continuous mobility formulation, then $m > 1$, and we have to multiply each additive term of $k_{0,r}^{(4)}$, $r = 1, \dots, m$ with the probability of selecting speed $z_r = r\delta v$, (i.e., $\nu_{r|i',j}$) and $\frac{1}{z_r}$ for the movement epoch that passes through cell c_0 , as it is shown by the formulation of $k_{i,r}^{(d)}$ in (22). Observe that, for all choices of V , the term $\sum_{r=1}^m k_{i,r}^{(d)}$ corresponds to the expected time spent over cell c_i while moving between two randomly picked cells that are drawn from the distributions $\varphi_{i'}$ in (10) and $\tau_{j|i'}$ in (7), respectively.

Next we proceed to the long-run analysis of the continuous- d mobility formulation. At first, recall that in this case since movement directions are restricted to four or six different directions, the path followed during a movement epoch between the points $X_s \in R$ and $X_d \in R$ will be composed two or one line segments each directed towards one of the available directions γ_i in (6), $i = 0, \dots, d-1$. Thus, in order to keep the formulation of this case separate from the exact model, where movement epochs occur on a single directed line segment that can have any direction, let the random variables $X^{(d)}(t) = (X_1^{(d)}(t), X_2^{(d)}(t))$ and $\tilde{V}^{(d)}(t)$, where d is either four or six, denote the location and the speed of a mobile terminal at time t , respectively. Note that $X^{(d)}(t) \in R$, and since the mobile can be in moving or pausing modes at any point in time, $\tilde{V}^{(d)}(t)$ is either equal to 0, or in the range $[v_{\min}, v_{\max}]$.

Now let $X^{(d)} = (X_1^{(d)}, X_2^{(d)})$ and $\tilde{V}^{(d)}$ denote the random variables having the long-run distribution of $X^{(d)}(t)$ and $\tilde{V}^{(d)}(t)$, respectively. Recall that in the discretized version of the mobility formulation, we assumed the random variables $X^{(d)}(t)$ and $\tilde{V}^{(d)}(t)$ to take only discrete values, and in Lemma 3, provided the long-run proportion of times that a mobile stays in cell c_i , (i.e., $p_i^{(d)}$ in (20)), and possesses speed z_r (i.e., $\psi_r^{(d)}$ in (21)). Therefore, in order to derive the distributions of $X^{(d)}$ and $\tilde{V}^{(d)}$, we need to focus on the limiting behavior of the discrete distributions given by Lemma 3 as discretization parameters n and m approaches infinity.

As an illustration of the methodology that is going to be applied during this transition, let's concentrate on the simple mobility formulation whose discretized version is depicted in Fig. 2.(a). Recall that, in that simple model $V = v$ (i.e., deterministic) and the other mobility characterization parameters can be arbitrary. Now for the discretized case, let $P_n^{(d)}(\frac{a}{2})$ denote the long-run proportion of time mobile is located in the region $R(\frac{a}{2}) = [0, \frac{a}{2}] \times [0, \frac{a}{2}]$. Hence, if $d = 4$ and $n = 4$, we have

$$P_4^{(4)}(\frac{a}{2}) = p_0^{(4)} \quad (28)$$

where $p_0^{(4)}$ is defined by (26). Notice that in this formulation the discretization parameter m is skipped because since $V = v$, and $m = 1$.

Next, the important question is what will be the limiting form of $P_n^{(d)}(\frac{a}{2})$ in (28) as $n \rightarrow \infty$. Hence, if we assume $n = 16$, then discretized region given in Fig. 2.(a) will be transformed to form given in Fig. 2.(b). By applying Lemma

3 we have

$$P_{16}^{(4)}(\frac{a}{2}) = \frac{\sum_{c_i \in \tilde{R}(\frac{a}{2})} \varphi_i (1 - \tau_{i|i}) E[T_{p_i}] + \sum_{c_i \in \tilde{R}(\frac{a}{2})} k_{i,1}^{(4)}}{N_{16,1}^{(4)}}, \quad (29)$$

where $\tilde{R}(\frac{a}{2}) = \{c_0, c_1, c_4, c_5\}$, that is, the set of discrete cells located on the region $R(\frac{a}{2})$.

Now based on the interpretation of $k_{i,r}^{(d)}$ in (22), the term $\sum_{c_i \in \tilde{R}(\frac{a}{2})} k_{i,1}^{(4)}$ corresponds to the average time spent over $R(\frac{a}{2})$ while moving between randomly picked two cells. Notice that both of those cells or one of them can be also belong to $\tilde{R}(\frac{a}{2})$. Hence we reach to the following:

$$\sum_{c_i \in \tilde{R}(\frac{a}{2})} k_{i,1}^{(4)} = \sum_{c_j \in \tilde{R}} \sum_{c_{i'} \in \tilde{R}} \varphi_{i'} \tau_{j|i'} P_{(\frac{a}{2})}(i', j) \frac{1}{v} J_{(\frac{a}{2})}(i', j) \Delta c^{(d)} \quad (30)$$

where $P_{(\frac{a}{2})}(i', j)$ denotes the probability passing over the region $R(\frac{a}{2})$ while moving from $c_{i'}$ to c_j , and $J_{(\frac{a}{2})}(i', j)$ represents the number of discrete jumps over $R(\frac{a}{2})$ while moving. Notice that the term $J_{(\frac{a}{2})}(i', j) \Delta c^{(d)}$ represents the total distance traveled over $R(\frac{a}{2})$, which is required to calculate the average time spent.

Therefore, in order to obtain the limiting form of $P_n^{(d)}(\frac{a}{2})$ as $n \rightarrow \infty$, we need to derive the limiting expression of the double summation given in (30) which requires a proper formulation of $P_{(\frac{a}{2})}(i', j)$ and $J_{(\frac{a}{2})}(i', j)$.

Thus, we now focus on the formalization of the observations we mentioned above. In order to keep our formulation as simple as possible, we concentrate on deriving the long-run distributions of the continuous-4 (i.e., $d = 4$) and continuous-6 (i.e., $d = 6$) mobility formulations over square and hexagonal mobility terrains of side length a , respectively. Denote these terrains with the generic notation $R^{(d)}(a)$, where d is substituted by 4 if it is a square, else by 6 (i.e., hexagon). Also, to describe long-run location distribution consistently with d and the shape of mobility terrain (i.e., $R^{(d)}(a)$), we focus on defining the probability mass function (pmf) of $X^{(d)}$ over a square subregion in $R^{(4)}(a)$, and a hexagonal subregion in $R^{(6)}(a)$. Let $R^{(d)}(x, b)$ denote these subregions, which is a square if $d = 4$, and a hexagon if $d = 6$, with center $x \in R^{(d)}(a)$ and side length b such that $R^{(d)}(x, b) \subseteq R^{(d)}(a)$. In Fig. 3, we provided illustrations of $R^{(4)}(a)$ and $R^{(4)}(x, b)$. We also denote by $\mathcal{S}^{(d)}(a, b)$ the set of all nonintersecting $R^{(d)}(x, b) \subseteq R^{(d)}(a)$.

In addition to the these notations, let $L^{(d)}(p, x_s, x_d, x, b)$ denote the length of the total distance traveled over the subregion $R^{(d)}(x, b)$ for a movement epoch that occurs between the points x_s and x_d , and passes through $R^{(d)}(x, b)$ with probability p , which can be equal to 1, 1/2, or 0 for the continuous- d mobility formulation. In Fig. 3, we depict $L^{(4)}(p, x_s, x_d, x, b)$ for example movement epochs. Finally, we define

$$\begin{aligned} S^{(d)}(p, x_d, x, b) \\ = \{x_s | x_s \in R^{(d)}(a), L^{(d)}(p, x_s, x_d, x, b) \neq 0\} \end{aligned} \quad (31)$$

Based on the notations given in the preceding two paragraphs, we are now ready to state the main theorem of this section.

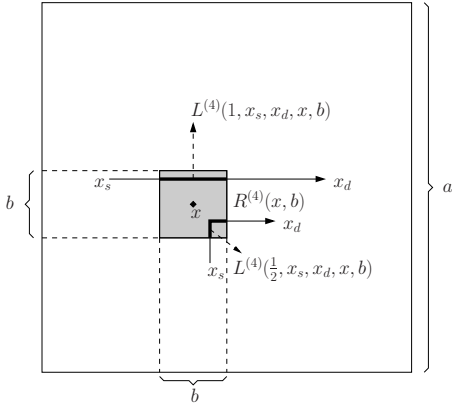


Fig. 3. Illustrations of $R^{(4)}(a)$, $R^{(4)}(x, b)$, and $L^{(4)}(p, x_s, x_d, x, b)$.

Theorem 1: For the mobile terminal, whose mobility pattern is characterized by the continuous- d mobility formulation over the mobility terrain $R^{(d)}(a)$, $d = 4, 6$, let $F_{X^{(d)}}(x, a, b)$ denote probability mass function of $X^{(d)}$ over the subregion $R^{(d)}(x, b) \subseteq R^{(d)}(a)$. Also, let $f_{\tilde{V}^{(d)}}$ denote the pdf of $\tilde{V}^{(d)}$.

If the pdf $f_{X_s}(x_d)$ can be uniquely determined from the integral equation (9), and $E[T_p|X_s = x_s] < \infty$, $\forall x_s \in R^{(d)}(a)$, and $f_{V|X_s, X_d} > 0$, $\forall v \in [v_{\min}, v_{\max}]$, and $\forall x_s, x_d \in R^{(d)}(a)$, then

$$F_{X^{(d)}}(x, a, b) = \frac{E[T_p|X_s \in R^{(d)}(x, b)] \Pr\{X_s \in R^{(d)}(x, b)\} + \int_{v_{\min}}^{v_{\max}} K^{(d)}(x, v, b, a) dv}{E[T_p|X_s \in R^{(d)}(a)] + \hat{D}^{(d)}}, \quad (32)$$

and

$$f_{\tilde{V}^{(d)}}(\tilde{v}) = \begin{cases} \frac{E[T_p|X_s \in R^{(d)}(a)]\delta(\tilde{v})}{E[T_p|X_s \in R^{(d)}(a)] + \hat{D}^{(d)}}, & \tilde{v} = 0 \\ \frac{\sum_{R^{(d)}(x, b) \in S^{(d)}(a, b)} K^{(d)}(x, \tilde{v}, b, a)}{E[T_p|X_s \in R^{(d)}(a)] + \hat{D}^{(d)}}, & \tilde{v} \in [v_{\min}, v_{\max}] \end{cases} \quad (33)$$

where

$$K^{(d)}(x, v, b, a) = \int_{x_d \in R^{(d)}(a)} dx_d \left(\int_{x_s \in S^{(d)}(1, x_d, x, b)} dx_s k^{(d)}(1, x_s, x_d, x, v, b) + \frac{1}{2} \int_{x_s \in S^{(d)}(1/2, x_d, x, b)} dx_s k^{(d)}(1/2, x_s, x_d, x, v, b) \right), \quad (34)$$

$$k^{(d)}(p, x_s, x_d, x, v, b) = f_{X_s}(x_s) f_{X_d|X_s}(x_d|x_s) \frac{1}{v} f_{V|X_s, X_d}(v|x_s, x_d) L^{(d)}(p, x_s, x_d, x, b), \quad (35)$$

and

$$\hat{D}^{(d)} = \sum_{R^{(d)}(x, b) \in S^{(d)}(a, b)} \int_{v_{\min}}^{v_{\max}} dv K^{(d)}(x, v, b, a) \quad (36)$$

Proof: Refer to [8]. ■

We may note that the term $\int_{v_{\min}}^{v_{\max}} K^{(d)}(x, v, b, a) dv$, where $K^{(d)}(x, v, b, a)$ is given in (34), corresponds to the expected time spent over the region $R^{(d)}(x, b)$ while moving between the points X_s and X_d that are respectively drawn from the distributions f_{X_s} and $f_{X_d|X_s}$. Also, in order to formulate $L^{(d)}(p, x_s, x_d, x, b)$ and the region $S^{(d)}(p, x_d, x, b)$ explicitly

we need to partition $R^{(d)}(a)$ with respect to $R^{(d)}(x, b)$. Clearly this will increase the complexity of the results presented by Theorem 1. However since we are aimed at using the distributions of the continuous- d case to reach some conclusions about the exact case, we decided to keep the presentation of the results given by Theorem 1 as simple as possible.

Now, in view of the result given by Claim 1 for $\hat{D}_n^{(d)}$ in (25), if V (i.e., the speed for a movement epoch) is assumed to be independent from the distributions of X_s and X_d , then we get the following for $\hat{D}^{(d)}$ in (36):

$$\hat{D}^{(d)} = E\left[\frac{1}{V}\right] \bar{D}^{(d)} \quad (37)$$

where

$$\bar{D}^{(d)} = \int_{x_s \in R^{(d)}(a)} dx_s \int_{x_d \in R^{(d)}(a)} dx_d f_{X_s}(x_s) f_{X_d|X_s}(x_d|x_s) |x_s - x_d|^{(d)} \quad (38)$$

where $|x_s - x_d|^{(d)}$ represent the total distance traveled between the points $x_s = (x_{s1}, x_{s2})$ and $x_d = (x_{d1}, x_{d2})$ for the continuous- d mobility formulation. Clearly if $d = 4$, then

$$|x_s - x_d|^{(4)} = |x_{d1} - x_{s1}| + |x_{d2} - x_{s2}| \quad (39)$$

which is also known as the *Manhattan distance* [11]. Also, notice that $|x_s - x_d|^{(4)} > |x_s - x_d|^{(6)}$, $\forall x_s, x_d \in R$.

Finally, based on the definition of $\bar{D}^{(d)}$ in (38), the $E[\tilde{V}^{(d)}]$ will be given by the following even if the distribution of V is dependent on the distributions of X_s and X_d .

$$E[\tilde{V}^{(d)}] = \frac{\bar{D}^{(d)}}{E[T_p|X_s \in R^{(d)}(a)] + \hat{D}^{(d)}} \quad (40)$$

IV. CONTINUOUS MOBILITY FORMULATION

In this section, we concentrate on the long-run properties of the continuous mobility formulation. In order to be as generic as possible, the mobility terrain R is assumed to be rectangular defined by $R = [0, a_1] \times [0, a_2]$. Denote $X(t)$ and $\tilde{V}(t)$, respectively, as the location and speed of a mobile terminal at time t . Because we are interested in the long-run distributions, let X and \tilde{V} respectively denote the random variables having the long-run distribution of $X(t)$ and $\tilde{V}(t)$. Notice that the state spaces of X and $X^{(d)}$, and \tilde{V} and $\tilde{V}^{(d)}$ are the same but since the continuous- d mobility formulation puts restriction on the movement directions, their long-run speed and location distributions will be always different from each other.

Now as mentioned before, since d can be either equal to four or six, the results provided by Theorem 1 cannot be extended formally to cover the exact case that allows mobile to move at any direction. Therefore, we now concentrate on using the results of Theorem 1 to construct an approximation methodology for the long-run distributions of the original continuous case.

Hence, analogous to the definition of $R^{(d)}(x, b)$ inside $R^{(d)}(a)$ (see Fig. 3), we define the following rectangular subregion inside $R = [0, a_1] \times [0, a_2]$ for the continuous case:

$$R(x, \Delta x_1, \Delta x_2) = [x_1 - \frac{\Delta x_1}{2}, x_1 + \frac{\Delta x_1}{2}] \times [x_2 - \frac{\Delta x_2}{2}, x_2 + \frac{\Delta x_2}{2}] \quad (41)$$

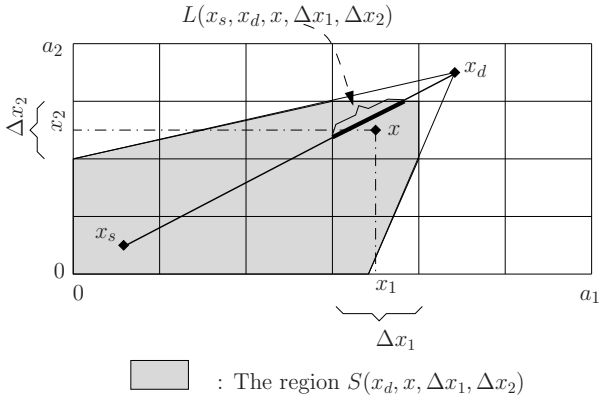


Fig. 4. Illustrations of $S(x_d, x, \Delta x_1, \Delta x_2)$ and $L(x_s, x_d, x, \Delta x_1, \Delta x_2)$ for the continuous mobility formulation.

where $x = (x_1, x_2)$, and Δx_1 and Δx_2 are selected such that $R(x, \Delta x_1, \Delta x_2) \subseteq R$. Also denote $\mathcal{S}(\Delta x_1, \Delta x_2)$ as the set of all nonintersecting $R(x, \Delta x_1, \Delta x_2) \subseteq R$.

Now notice that since the direction of movement is not restricted, a movement epoch that starts from a point x_s with destination x_d passes through the region $R(x, \Delta x_1, \Delta x_2)$ with probability one or zero. On the other hand, for the continuous- d case, movement epochs passes through $R^{(d)}(x, b)$ with probability 1, 1/2, or 0. Hence, if we denote the the distance traveled over $R(x, \Delta x_1, \Delta x_2)$ during a movement epoch by $L(x_s, x_d, x, \Delta x_1, \Delta x_2)$, the correspondent of $S^{(d)}(p, x_d, x, b)$ in (31) can be simply defined by the following for the original continuous case:

$$S(x_d, x, \Delta x_1, \Delta x_2) = \{x_s | x_s \in R, L(x_s, x_d, x, \Delta x_1, \Delta x_2) \neq 0\} \quad (42)$$

In Fig. 4, we illustrate $S(x_d, x, \Delta x_1, \Delta x_2)$ and the line segment $L(x_s, x_d, x, \Delta x_1, \Delta x_2)$ for a destination point x_d outside the region $R(x, \Delta x_1, \Delta x_2)$.

In view of these definitions, and from the conclusions of Theorem 1, we derive the following approximations for the long-run distributions of the original continuous case.

Approximation 1: For the mobile terminal, whose mobility pattern is characterized by the triplet $\langle f_{X_d|X_s}, f_{V|X_s, X_d}, f_{T_p|X_d} \rangle$, over the mobility terrain $R = [0, a_1] \times [0, a_2]$, let $F_X(x, \Delta x_1, \Delta x_2)$ denote probability mass function of X over the subregion $R(x, \Delta x_1, \Delta x_2)$ in (41). Also, let $f_{\tilde{V}}$ denote the pdf of \tilde{V} .

If the pdf $f_{X_s}(x_d)$ can be uniquely determined from the integral equation (9), and $E[T_p|X_s = x_s] < \infty, \forall x_s \in R$, and $f_{V|X_s, X_d} > 0, \forall v \in [v_{\min}, v_{\max}]$, and $\forall x_s, x_d \in R$, then $F_X(x, \Delta x_1, \Delta x_2)$ and $f_{\tilde{V}}$ are approximated by

$$F_X(x, \Delta x_1, \Delta x_2) \approx \frac{E[T_p|X_s \in R(x, \Delta x_1, \Delta x_2)] \Pr\{X_s \in R(x, \Delta x_1, \Delta x_2)\}}{E[T_p|X_s \in R] + \hat{D}} + \frac{\int_{v_{\min}}^{v_{\max}} K(x, v, \Delta x_1, \Delta x_2) dv}{E[T_p|X_s \in R] + \hat{D}} \quad (43)$$

and

$$f_{\tilde{V}}(\tilde{v}) \approx \begin{cases} \frac{E[T_p|X_s \in R]\delta(\tilde{v})}{E[T_p|X_s \in R] + \hat{D}}, & \tilde{v} = 0 \\ \frac{\sum_{R(x, \Delta x_1, \Delta x_2) \in \mathcal{S}(\Delta x_1, \Delta x_2)} K(x, \tilde{v}, \Delta x_1, \Delta x_2)}{E[T_p|X_s \in R] + \hat{D}}, & \tilde{v} \in [v_{\min}, v_{\max}] \end{cases}, \quad (44)$$

where

$$K(x, v, \Delta x_1, \Delta x_2) = \int_{x_d \in R} dx_d \int_{x_s \in \mathcal{S}(x_d, x, \Delta x_1, \Delta x_2)} dx_s k(x_s, x_d, x, v, \Delta x_1, \Delta x_2), \quad (45)$$

$$k(x_s, x_d, x, v, \Delta x_1, \Delta x_2) = f_{X_s}(x_s) f_{X_d|X_s}(x_d|x_s) \frac{1}{v} f_{V|X_s, X_d}(v|x_s, x_d) L(x_s, x_d, x, \Delta x_1, \Delta x_2), \quad (46)$$

and

$$\hat{D} = \sum_{R(x, \Delta x_1, \Delta x_2) \in \mathcal{S}(\Delta x_1, \Delta x_2)} \int_{v_{\min}}^{v_{\max}} dv K(x, v, \Delta x_1, \Delta x_2) \quad (47)$$

Now recall that for the continuous- d mobility formulation, if V is assumed to be independent from X_s and X_d , then $\hat{D}^{(d)} = E[\frac{1}{\tilde{V}}] \bar{D}^{(d)}$, where $\bar{D}^{(d)}$ is given by (38). Based on this observation we state the following approximation:

Approximation 2: If the distribution of V is assumed to be independent from X_s and X_d , then the \hat{D} in (47) is approximated by

$$\hat{D} \approx E[\frac{1}{\tilde{V}}] \bar{D} \quad (48)$$

where

$$\bar{D} = \int_{x_s \in R} dx_s \int_{x_d \in R} dx_d f_{X_s}(x_s) f_{X_d|X_s}(x_d|x_s) |x_s - x_d| \quad (49)$$

where $|x_s - x_d|$ denotes the euclidean distance between x_s and x_d .

In addition, from the formulation of $E[\tilde{V}^{(d)}]$ in (40), we reach to the following approximation.

Approximation 3: The expected value of \tilde{V} with the pdf defined by (44) is approximated by

$$E[\tilde{V}] \approx \frac{\bar{D}}{E[T_p|X_s \in R] + \hat{D}} \quad (50)$$

Having defined an approximation to $E[\tilde{V}]$ for the most generic case, we note that the analytical work presented in [7] also derives $f_{\tilde{V}}$ and $E[\tilde{V}]$ for a class of mobility models where the speed of a movement epoch is selected independently from the distance that is going to be traveled for that epoch. In order to be able to compare our results with the ones given in that paper, we must consider the scenarios that the triplet $\langle f_{X_d}, f_V, f_{T_p} \rangle$ is enough for mobility characterization, that is, distributions of X_d and T_p are independent from X_s , and V is independently selected from X_s and X_d . Hence, after simplifying $f_{\tilde{V}}$ in (44), and $E[\tilde{V}]$ in (50), we get

$$f_{\tilde{V}}(v) \approx \begin{cases} \frac{E[T_p]\delta(v)}{E[T_p] + E[\frac{1}{\tilde{V}}]\bar{D}}, & v=0 \\ \frac{\frac{1}{v} f_V(v)\bar{D}}{E[T_p] + E[\frac{1}{\tilde{V}}]\bar{D}}, & v \in [v_{\min}, v_{\max}] \end{cases}, \quad E[\tilde{V}] \approx \frac{\bar{D}}{E[T_p] + E[\frac{1}{\tilde{V}}]\bar{D}} \quad (51)$$

where $\delta(v)$ is defined as the direc delta function. The above formulation of $f_{\tilde{V}}$ and $E[\tilde{V}]$ are consistent with the ones given in [7]. Hence, our approximations for $f_{\tilde{V}}$ and $E[\tilde{V}]$ becomes exact for the mobility characterizations done by $\langle f_{X_d}, f_V, f_{T_p} \rangle$.

We should also note that, the results presented by Approximations 1, 2, and 3, becomes exact for a mobility modeling that restricts the available movement directions to 4 or 6 different choices that are exactly defined by γ_i in equation (6). As an application of this case, consider a mobility scenario where mobiles are only allowed to move on the grids over the mobility terrain.

We finally note that, since we can only prove the limited direction case, we can never state that these approximations are highly accurate for all possible mobility scenarios defined by the triplet $\langle f_{X_d|X_s}, f_{V|X_s, X_d}, f_{T_p|X_d} \rangle$. Fundamentally, their accuracy is dependent on the frequency of the movement epochs that is targeted to a destination point with a moving direction outside the directions γ_i in (6), where $i = 4, 6$. Hence, in Section V, we concentrate on the applicability and accuracy of our approximations for some example cases that allows mobiles to move at any direction when traveling towards the destination point. The methodology we follow in Section V to analyze the accuracy of the approximations can be also applied to analyze other example mobility cases.

A. Approximation to the pdf of long-run location distribution

Before proceeding further, we now focus on simplifying the results of Approximation 1 to derive an approximation to the pdf of long-run location distribution in closed form. Hence, let f_X denote the pdf of X , that is, the random variable having the long-run distribution of $X(t)$. It then follows from the definition given in [12] for the pdf of bivariate random variables that

$$f_X(x) = \lim_{\substack{\Delta x_1 \rightarrow 0 \\ \Delta x_2 \rightarrow 0}} \frac{F_X(x, \Delta x_1, \Delta x_2)}{\Delta x_1 \Delta x_2} \quad (52)$$

At this point, the important question is, given the triplet $\langle f_{X_d|X_s}, f_{V|X_s, X_d}, f_{T_p|X_d} \rangle$, whether it is possible to find a closed form expression for the term $K(x, v, \Delta x_1, \Delta x_2)$ in (45) so that the above limit can be taken explicitly. If this can be done, then we can state an approximation to $f_X(x)$ in closed form.

To answer this question, we first concentrate on a simple scenario where X_d is uniformly distributed over R for a given X_s , and V is characterized by f_V . Obviously for this case, $K(x, v, \Delta x_1, \Delta x_2)$ in (45) simplifies to

$$\begin{aligned} & K(x, v, \Delta x_1, \Delta x_2) \\ &= \frac{f_V(v)}{(a_1 a_2)^2 v} \int_{x_d \in R} dx_d \int_{x_s \in S(x_d, x, \Delta x_1, \Delta x_2)} dx_s L(x_s, x_d, x, \Delta x_1, \Delta x_2) \end{aligned} \quad (53)$$

Therefore, to be able to derive a closed form expression for $K(x, v, \Delta x_1, \Delta x_2)$, the integrand $L(x_s, x_d, x, \Delta x_1, \Delta x_2)$ must be expressible in terms of a function that can be analytically integrated over the given integration region.

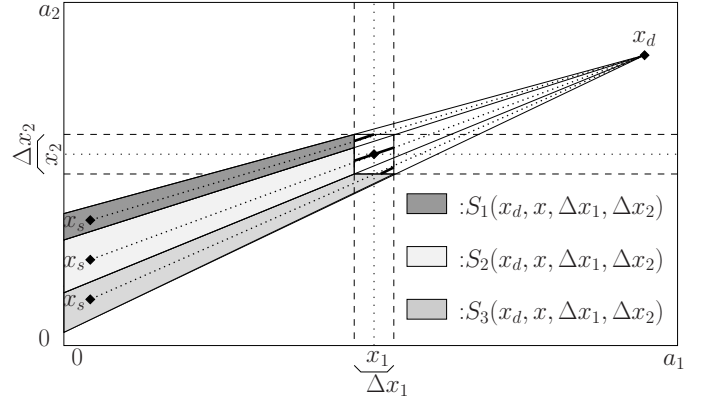


Fig. 5. Partitioning the region $S(x_d, x, \Delta x_1, \Delta x_2)$.

Now from the definition of $L(x_s, x_d, x, \Delta x_1, \Delta x_2)$, and also from Fig. 4, observe that

$$L(x_s, x_d, x, \Delta x_1, \Delta x_2) = (g(x_s, x_d, x, \Delta x_1, \Delta x_2))^{1/2} \quad (54)$$

for a function $g(x_s, x_d, x, \Delta x_1, \Delta x_2)$ that is piecewise continuous on $S(x_d, x, \Delta x_1, \Delta x_2)$ for given $x_d \in R$. Clearly, the analytical integration of $L(x_s, x_d, x, \Delta x_1, \Delta x_2)$ in (54) over the given 4-dimensional integration region (see (53)) is complicated. Hence, we conclude that obtaining a closed form expression for $K(x, v, \Delta x_1, \Delta x_2)$ even for the simplest of all possible mobility characterization parameters is nearly impossible.

However, if some exceptional choices of $x_s = (x_{s_1}, x_{s_2})$ and $x_d = (x_{d_1}, x_{d_2})$ are not taken into consideration, for example, suppose that $x_s, x_d \notin R(x, \Delta x_1, \Delta x_2)$, $|x_{d_1} - x_{s_1}| > \frac{\Delta x_1}{2}$, and $|x_{d_2} - x_{s_2}| > \frac{\Delta x_2}{2}$, then $L(x_s, x_d, x, \Delta x_1, \Delta x_2)$ will be expressible in terms of an easily integrable function for some mobility characterization choices.

To be more precise, on the rectangular mobility terrain $R = [0, a_1] \times [0, a_2]$ assume $x_{d_1} > x_1 + \frac{\Delta x_1}{2}$ and $x_{d_2} > x_2 + \frac{\Delta x_2}{2}$. Furthermore, let $\ell_R(x_1)$ denote the line segment joining the points x_d and $(x_1 + \frac{\Delta x_1}{2}, x_2 - \frac{\Delta x_2}{2})$, and assume $\ell_R(0) > 0$. In Fig. 5, we provided a visualization of these assumptions. Notice that this special case also implies $|x_{d_1} - x_{s_1}| > |x_{d_2} - x_{s_2}|$. In addition, consider the partitioning of the subregion $S(x_d, x, \Delta x_1, \Delta x_2)$ into three subregions as shown in Figure 5, and denote $L_r(x_s, x_d, x, \Delta x_1, \Delta x_2)$, $r = 1, 2, 3$, as the distance traveled over $R(x, \Delta x_1, \Delta x_2)$ when $x_s \in S_r(x_d, x, \Delta x_1, \Delta x_2)$. Next, formulating $L_r(x_s, x_d, x, \Delta x_1, \Delta x_2)$ explicitly we get

$$\begin{aligned} & L_r(x_s, x_d, x, \Delta x_1, \Delta x_2) \\ &= \begin{cases} |x_d - x_s| \frac{\Delta x_1}{x_{d_1} - x_{s_1}}, & r=2 \\ |x_d - x_s| \left(\frac{x_2 + c_r \frac{\Delta x_2}{2} - x_{s_2}}{x_{d_2} - x_{s_2}} - \frac{x_1 + c_r \frac{\Delta x_1}{2} - x_{s_1}}{x_{d_1} - x_{s_1}} \right), & r=1,3 \end{cases} \end{aligned} \quad (55)$$

where $c_1 = 1$ and $c_3 = -1$.

Before we proceed further, it should be noted that, for the formulation that assumes $x_{d_1} > x_1 + \frac{\Delta x_1}{2}$ and $x_{d_2} > x_2 + \frac{\Delta x_2}{2}$, if we had concentrated on the case that only allows $|x_{d_2} - x_{s_2}| > |x_{d_1} - x_{s_1}|$, and had partitioned $S(x_d, x, \Delta x_1, \Delta x_2)$ in the same way as we did in Fig. 5, then

the $L_r(x_s, x_d, x, \Delta x_1, \Delta x_2)$, $r = 1, 3$, would be also defined by (55). However, if $r = 2$, then

$$L_2(x_s, x_d, x, \Delta x_1, \Delta x_2) = |x_d - x_s| \frac{\Delta x_2}{x_{d_2} - x_{s_2}}, \quad (56)$$

which is expected intuitively.

Now returning back to case that is constructed according to the assumption $|x_{d_1} - x_{s_1}| > |x_{d_2} - x_{s_2}|$, it is clear that $L_2(x_s, x_d, x, \Delta x_1, \Delta x_2) > L_r(x_s, x_d, x, \Delta x_1, \Delta x_2)$, $r = 1, 3$ (also observe it from Fig. 5). Hence, concentrating on $L_2(x_s, x_d, x, \Delta x_1, \Delta x_2)$ observe the following:

$$L_2(x_s, x_d, x, \Delta x_1, \Delta x_2) = \Delta x_1 \sqrt{1 + \frac{(x_{d_2} - x_{s_2})^2}{(x_{d_1} - x_{s_1})^2}}, \quad (57)$$

Obviously as the difference between $|x_{d_1} - x_{s_1}|$ and $|x_{d_2} - x_{s_2}|$ increases, the term $\frac{(x_{d_2} - x_{s_2})^2}{(x_{d_1} - x_{s_1})^2}$ converges to zero. Hence, we can state the following:

$$L_2(x_s, x_d, x, \Delta x_1, \Delta x_2) \approx \Delta x_1 \quad (58)$$

Finally, since $L_2(x_s, x_d, x, \Delta x_1, \Delta x_2)$ is always more dominant than $L_r(x_s, x_d, x, \Delta x_1, \Delta x_2)$, $r = 1, 3$, we conclude the following approximation.

$$L(x_s, x_d, x, \Delta x_1, \Delta x_2) \approx \begin{cases} \Delta x_1, & |x_{d_1} - x_{s_1}| > |x_{d_2} - x_{s_2}| \\ \Delta x_2, & |x_{d_1} - x_{s_1}| < |x_{d_2} - x_{s_2}| \end{cases} \quad (59)$$

As a result, if mobility model is simple enough to state $K(x, v, \Delta x_1, \Delta x_2)$ as in (53), and if the above substitution for $L(x_s, x_d, x, \Delta x_1, \Delta x_2)$ is used, then the result of Approximation 1 can be simplified to derive an approximation for f_X in closed form after tedious symbolic integrations. We also concentrate on the applicability of this statement in the next section.

V. EXAMPLE SCENARIOS

Example 1: The random waypoint model proposed in [4], which is commonly used to model node movement by the performance analysis studies for wireless ad hoc networks, can be considered as the simplest nontrivial case for the mobility characterizations that can be analyzed according to the triplet $\langle f_{X_d|X_s}, f_{V|X_s, X_d}, f_{T_p|X_d} \rangle$. For this model, the distributions of X_d and V are assumed to be uniform in the regions R and $[v_{\min}, v_{\max}]$, respectively. Moreover, the distribution of T_p is considered to be the same at all destinations. Therefore, for the rectangular mobility terrain $R = [0, a_1] \times [0, a_2]$, we simply have

$$f_{X_s}(x_d) = \begin{cases} \frac{1}{a_1 a_2}, & \text{if } x_d \in [0, a_1] \times [0, a_2] \\ 0, & \text{otherwise} \end{cases} \quad (60)$$

Hence, from Approximations 1 and 2 we reach the following approximation for the pmf of X over $R(x, \Delta x_1, \Delta x_2)$ in (41):

$$F_X(x, \Delta x_1, \Delta x_2) \approx \frac{E[T_p] \Delta x_1 \Delta x_2 + E[\frac{1}{V}] K_X(x, \Delta x_1, \Delta x_2)}{E[T_p] + E[\frac{1}{V}] \bar{D}} \quad (61)$$

where

$$K_X(x, \Delta x_1, \Delta x_2) = \int_{x_d \in R} dx_d \int_{x_s \in S(x_d, x, \Delta x_1, \Delta x_2)} L(x_s, x_d, x, \Delta x_1, \Delta x_2) \quad (62)$$

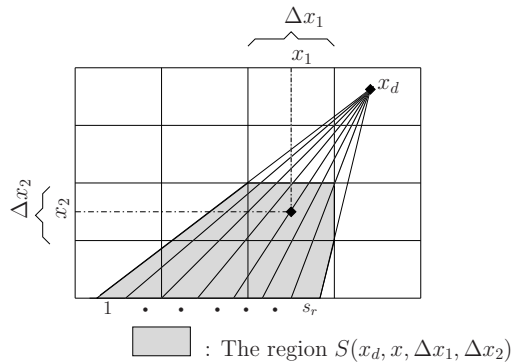


Fig. 6 Partitioning of $S(x_d, x, \Delta x_1, \Delta x_2)$ into s_r subregions for a given x_d .

where $E[\frac{1}{V}] = \frac{\ln(\frac{v_{\max}}{v_{\min}})}{(v_{\max} - v_{\min})}$, and \bar{D} is given by (49). In addition, $f_{\bar{V}}$ and $E[\bar{V}]$ can be derived respectively from the equations in (51).

In order to assess the accuracy of the approximation we stated for $F_X(x, \Delta x_1, \Delta x_2)$ by equation (61) for the random waypoint model, we will now focus on the task of evaluating $F_X(x, \Delta x_1, \Delta x_2)$ in (61) numerically for all $R(x, \Delta x_1, \Delta x_2) \in \mathcal{S}(\Delta x_1, \Delta x_2)$, and comparing them with the results derived from the simulation of the random waypoint mobility model.

Hence, observe first that to generate an approximation to $F_X(x, \Delta x_1, \Delta x_2)$ from (61) for a given $R(x, \Delta x_1, \Delta x_2)$, we need to evaluate $K_X(x, \Delta x_1, \Delta x_2)$ numerically in (62), which is defined by a 4-dimensional integral. Obviously, the accuracy of a result that can be derived from a numerical integration methodology is dependent on the *smoothness* of the integrand over the integration region [13]. Therefore, to increase the accuracy of our numerical experiments, we partition the region $S(x_d, x, \Delta x_1, \Delta x_2)$ into s_r subregions, where $s_r \geq 1$, so that the integrand $L(x_s, x_d, x, \Delta x_1, \Delta x_2)$ (see (62)) evaluated for a fixed x_d deviates less for all of the x_s that belongs to those subregions. In Fig. 6, we illustrated this partitioning methodology for a given x_d . Next, to evaluate the 4-dimensional integrals for each of these subregions, we first transformed them to an integral over a hypercube [13]. Then, each of the resulting integrals are evaluated by repeated one-dimensional integrations according to the Gauss' Formula [14]. Clearly, this is not "economical", however, it is required in order to evaluate the accuracy of our approximation. The program implementing this methodology is designed in a generic form in order to also capture different mobility characterization parameters, and it is available from authors.

In order to assess the accuracy of the approximation to $F_X(x, \Delta x_1, \Delta x_2)$, a simple simulation model is developed consisting of a single node moving according to the random waypoint mobility profile. In this model, during each simulation run, the node travels for n_e number of movement epochs. For each movement epoch, the time spent at each $R(x, \Delta x_1, \Delta x_2) \in \mathcal{S}(\Delta x_1, \Delta x_2)$, while passing through it or pausing at it, is exactly calculated, and added to the total time spent at the subregion $R(x, \Delta x_1, \Delta x_2)$ for the whole simulation run. At the end of the run, $F_X(x, \Delta x_1, \Delta x_2)$ is derived by normalizing the total time spent at $R(x, \Delta x_1, \Delta x_2)$ to the total

a_2	1.237	0.425	0.352	0.4	0.355	0.323	0.345	1.231	
$\frac{a_2}{6}$	0.563	0.212	0.223	0.194	0.216	0.259	0.241	0.494	
$\frac{a_2}{6}$	0.491	0.254	0.133	0.143	0.167	0.246	0.256	0.41	
$\frac{a_2}{6}$	0.688	0.183	0.127	0.171	0.25	0.2	0.215	0.501	
$\frac{a_2}{6}$	0.632	0.226	0.226	0.221	0.259	0.205	0.159	0.709	
$\frac{a_2}{6}$	1.04	0.316	0.385	0.346	0.353	0.291	0.468	1.291	
0	0	$\frac{a_1}{8}$	$\frac{2a_1}{8}$	$\frac{3a_1}{8}$	$\frac{4a_1}{8}$	$\frac{5a_1}{8}$	$\frac{6a_1}{8}$	$\frac{7a_1}{8}$	a_1

(a)

a_2	1.503	0.092	1.72	2.476	2.436	1.691	0.172	1.573	
$\frac{a_2}{6}$	0.388	0.536	0.331	0.865	0.844	0.295	0.566	0.47	
$\frac{a_2}{6}$	0.189	0.180	0.33	0.301	0.326	0.442	0.182	0.377	
$\frac{a_2}{6}$	1.432	0.11	0.323	0.329	0.406	0.395	0.142	1.353	
$\frac{a_2}{6}$	4.07	0.551	0.328	0.839	0.802	0.348	0.483	3.805	
$\frac{a_2}{6}$	3.862	0.201	1.752	2.427	2.434	1.659	0.048	3.868	
0	0	$\frac{a_1}{8}$	$\frac{2a_1}{8}$	$\frac{3a_1}{8}$	$\frac{4a_1}{8}$	$\frac{5a_1}{8}$	$\frac{6a_1}{8}$	$\frac{7a_1}{8}$	a_1

(b)

Fig. 7. $E_X^{(S,A)}(b^{(1)}, b^{(2)})$ for Example 1 ($a_1 = 1200$, $a_2 = 900$, $b_1^{(1)} = i a_1/8$, $i = 0, \dots, 7$, $b_2^{(1)} = b_1^{(1)} + a_1/8$, $b_1^{(2)} = j a_2/6$, $j = 0, \dots, 5$, $b_2^{(2)} = b_1^{(2)} + a_2/6$, $v_{\min} = 1$ m/s, $v_{\max} = 20$ m/s, $T_p = U[0, 30]$ sec).

run time of the experiment. n_r independent replications of this experiment is run, and the final $F_X(x, \Delta x_1, \Delta x_2)$ is obtained by averaging the results of these runs. Also, at the beginning of each replication, the initial location, and speed and pause time distributions of the node is determined according to the methodology explained in [6] for the efficient and reliable simulation of random waypoint mobility model.

Now to be able to represent a comparison of the results obtained from (61), and from the simulation model we described above, consider the region $[b_1^{(1)}, b_2^{(1)}] \times [b_1^{(2)}, b_2^{(2)}] \subseteq R$ where $b_i^{(1)}$, $i = 1, 2$, and $b_j^{(2)}$, $j = 1, 2$, are multipliers of Δx_1 and Δx_2 , respectively. Notice that if $P_X(b^{(1)}, b^{(2)})$ denotes the probability of the mobile terminal to be located over the region $[b_1^{(1)}, b_2^{(1)}] \times [b_1^{(2)}, b_2^{(2)}]$ at the long-run, then $P_X(b^{(1)}, b^{(2)})$ can be easily derived by accumulating all of the $F_X(x, \Delta x_1, \Delta x_2)$ such that $R(x, \Delta x_1, \Delta x_2) \subset [b_1^{(1)}, b_2^{(1)}] \times [b_1^{(2)}, b_2^{(2)}]$. Hence, let $P_X^{(A)}(b^{(1)}, b^{(2)})$ and $P_X^{(S)}(b^{(1)}, b^{(2)})$ respectively denote the correspondent of $P_X(b^{(1)}, b^{(2)})$ obtained from (61) (i.e., Approximation 1) and from the simulation model. Based on these notations, we define the following metric to assess the correctness of our conjecture for this mobility model.

$$E_X^{(S,A)}(b^{(1)}, b^{(2)}) = \frac{|P_X^{(S)}(b^{(1)}, b^{(2)}) - P_X^{(A)}(b^{(1)}, b^{(2)})|}{P_X^{(S)}(b^{(1)}, b^{(2)})}, \quad (63)$$

Finally, for our experiments, we considered a $[0, 1200]m \times [0, 900]m$ mobility terrain, and set the parameters of mobility as follows: $v_{\min} = 1m/s$, $v_{\max} = 20m/s$, and T_p is uniform over the range $[0, 30]sec$. Then, we chose $\Delta x_1 = \Delta x_2 = 5m$, and set $n_e = 10^7$, $n_r = 100$ for the simulation experiment, and evaluated $E_X^{(S,A)}(b^{(1)}, b^{(2)})$ for various choices of $b_i^{(1)}$ and $b_i^{(2)}$, $i = 1, 2$. The results are presented in Fig. 7.(a). Simulation results are acquired with a 95% confidence interval lower than 0.001. Since the percentage of error, (i.e., $E_X^{(S,A)}(b^{(1)}, b^{(2)}) \times 100$) is at most 1.29% we conclude that the application of the Approximation 1 to random waypoint mobility model is accurate.

Thus, using $F_X(x, \Delta x_1, \Delta x_2)$ in (61) we can obtain an

approximation to the pmf of $X = (X_1, X_2)$ over the subregion $R(x, \Delta x_1, \Delta x_2)$ numerically. With this knowledge at hand, we will now concentrate on finding $E[X_1]$, $E[X_2]$, and $Corr(X_1, X_2)$. Hence, we set $\Delta x_1 = \frac{a_1}{n_1}$ and $\Delta x_2 = \frac{a_2}{n_2}$ for some discretization parameters $n_1, n_2 \in \mathbf{Z}^+$, and define the discrete bivariate random variable $X^* = (X_1^*, X_2^*)$ with the finite state space

$$\mathcal{S}^* = \left\{ \frac{\Delta x_1}{2}, \frac{3\Delta x_1}{2}, \dots, \frac{(2n_1-1)\Delta x_1}{2} \right\} \times \left\{ \frac{\Delta x_2}{2}, \frac{3\Delta x_2}{2}, \dots, \frac{(2n_2-1)\Delta x_2}{2} \right\} \quad (64)$$

to denote the subregion $R(x^*, \Delta x_1, \Delta x_2)$ in (41), where $x^* \in \mathcal{S}^*$, that the mobile is located at the long-run. Clearly, as $n_1 \rightarrow \infty$ and $n_2 \rightarrow \infty$, X^* converges to the continuous bivariate random variable X .

Evaluating the distribution of X^* from $F_X(x, \Delta x_1, \Delta x_2)$ in (61) we obtained $E[X_1^*]$, $E[X_2^*]$, and $Corr(X_1^*, X_2^*)$ numerically for several different parameter choices for the random waypoint mobility model. For all of the scenarios we considered, we set n_1 and n_2 sufficiently large enough to closely approximate $X = (X_1, X_2)$ with $X^* = (X_1^*, X_2^*)$, and observed the following:

$$E[X_1^*] = \frac{a_1}{2}, \quad E[X_2^*] = \frac{a_2}{2}, \quad Corr(X_1^*, X_2^*) = 0 \quad (65)$$

The simulation studies presented in [15], [16] points out that the long-run location distribution of the random waypoint mobility model is more accumulated at the center of the mobility terrain. More importantly, it is symmetric with respect to center. Therefore, obtaining $E[X_1^*]$ and $E[X_2^*]$ as in (65) is expected. However, the result for $Corr(X_1^*, X_2^*) = 0$ is not observed before. In fact, our numerical experiments showed that X_1^* and X_2^* are not independent.

It should also be noted that analytical work presented in [5] for the spatial node distribution generated by this mobility model concentrates on the case where $R = [0, a] \times [0, a]$, V is deterministic with parameter v , and $E[T_p] = 0$, and formulates the long-run cumulative distribution function over a region with an area of δ^2 . If we substitute $E[1/V]$ with $\frac{1}{v}$, and $E[T_p] = 0$, and assume $\Delta x_1 = \Delta x_2 = \delta$, and $a_1 = a_2$, the formulation of the approximation we defined by (61) for

$F_X(x, \Delta x_1, \Delta x_2)$ becomes consistent with the formulation of the cumulative distribution function given in [5].

We now focus on applying the approximation we defined by (59) for $L(x_s, x_d, x, \Delta x_1, \Delta x_2)$ to derive an approximation to $f_X(x)$ in (52) (i.e., the pdf of X). First, notice from the formulation of $K_X(x, \Delta x_1, \Delta x_2)$ in (62) that when this approximation is used, the integration of the integrand over the region $S(x_d, x, \Delta x_1, \Delta x_2)$, will be equal to Δx_1 or Δx_2 times the area of the region $S(x_d, x, \Delta x_1, \Delta x_2)$. Hence, by partitioning the boundaries of the 4-dimensional integration that formulates $K_X(x, \Delta x_1, \Delta x_2)$ according to the condition $|x_{d_1} - x_{s_1}| > |x_{d_2} - x_{s_2}|$ and its counterpart appropriately, we obtained a closed form expression for (62). Finally, evaluating the limit $\frac{F_X(x, \Delta x_1, \Delta x_2)}{\Delta x_1 \Delta x_2}$ as $\Delta x_1 \rightarrow 0$ and $\Delta x_2 \rightarrow 0$, we reached the following approximation for f_X :

$$f_X(x) \approx \tilde{f}_X(x) \quad (66)$$

where

$$\tilde{f}_X(x) = \frac{E[T_p] \frac{1}{a_1 a_2} + E[\frac{1}{V}] k(x) / \tilde{N}}{E[T_p] + E[\frac{1}{V}] \bar{D}} \quad (67)$$

where

$$k(x) = \begin{cases} k_1(x) + k_4(x) + k_6(x) + k_8(x), & 0 < x_1 < \frac{a_1}{2}, 0 < x_2 < \frac{a_2 x_1}{a_1} \\ k_1(x) + k_4(x) + k_6(x) + k_8(x), & \frac{a_1}{2} < x_1 < a_1, 0 < x_2 < a_2(1 - \frac{x_1}{a_1}) \\ k_2(x) + k_4(x) + k_5(x) + k_8(x), & 0 < x_1 < \frac{a_1}{2}, \frac{a_2 x_1}{a_1} < x_2 < a_2(1 - \frac{x_1}{a_1}) \\ k_1(x) + k_3(x) + k_6(x) + k_7(x), & \frac{a_1}{2} < x_1 < a_1, a_2(1 - \frac{x_1}{a_1}) < x_2 < \frac{a_2 x_1}{a_1} \\ k_2(x) + k_3(x) + k_5(x) + k_7(x), & 0 < x_1 < \frac{a_1}{2}, a_2(1 - \frac{x_1}{a_1}) < x_2 < a_2 \\ k_2(x) + k_3(x) + k_5(x) + k_7(x), & \frac{a_1}{2} < x_1 < a_1, \frac{a_2 x_1}{a_1} < x_2 < a_2 \end{cases} \quad (68)$$

where $x = (x_1, x_2)$, and $k_i(x)$, $i = 1, \dots, 8$ are defined by

$$\begin{aligned} k_1(x) &= \frac{(a_1 - x_1)x_2[2a_2x_1 + a_1(x_1 - x_2) + x_1x_2g_1(x)]}{2a_1^2a_2^2x_1} \\ k_2(x) &= \frac{x_1(a_2 - x_2)[2a_1x_2 + a_2(x_2 - x_1) - x_1x_2g_1(x)]}{2a_1^2a_2^2x_2} \\ k_3(x) &= \frac{(a_1 - x_1)(a_2 - x_2)[a_2(x_1 - a_1) + x_2(a_2 + 2a_1) + (a_1 - x_1)x_2g_2(x)]}{2a_1^2a_2^2x_2} \\ k_4(x) &= \frac{x_1x_2[(a_1 + 2a_2)(a_1 - x_1) - a_1x_2 - (a_1 - x_1)x_2g_2(x)]}{2a_1^2a_2^2(a_1 - x_1)} \\ k_5(x) &= \frac{x_1(a_2 - x_2)[a_1(a_1 - x_1 + x_2) + a_2(a_1 - 2x_1) - (a_1 - x_1)(a_2 - x_2)g_1(x)]}{2a_1^2a_2^2(a_1 - x_1)} \\ k_6(x) &= \frac{(a_1 - x_1)x_2[a_2(a_1 + a_2 + x_1) - (2a_1 + a_2)x_2 + (a_1 - x_1)(a_2 - x_2)g_1(x)]}{2a_1^2a_2^2(a_2 - x_2)} \\ k_7(x) &= \frac{(a_1 - x_1)(a_2 - x_2)[2a_2x_1 + a_1(x_1 + x_2 - a_2) + x_1(a_2 - x_2)g_2(x)]}{2a_1^2a_2^2x_1} \\ k_8(x) &= \frac{x_1x_2[a_2(2a_1 + a_2 - x_1) - (2a_1 + a_2)x_2 - x_1(a_2 - x_2)g_2(x)]}{2a_1^2a_2^2(a_2 - x_2)} \end{aligned}$$

where

$$g_1(x) = \log\left(\frac{x_1(a_2 - x_2)}{(a_1 - x_1)x_2}\right), \quad g_2(x) = \log\left(\frac{x_1x_2}{(a_1 - x_1)(a_2 - x_2)}\right) \quad (69)$$

and \tilde{N} is the normalization term given by

$$\tilde{N} = \left(\int_{x \in R} k(x) dx \right) / \bar{D} \quad (70)$$

It should be noted that since the term $L(x_s, x_d, x, \Delta x_1, \Delta x_2)$ is either substituted by Δx_1 or Δx_2 , the function $k(x)$ in (68) must be normalized in the region R so that $\tilde{f}_X(x)$ will be a probability density function.

In order to assess the validity of the approximation we presented by (66) we evaluated $P_X^{(A)}(b^{(1)}, b^{(2)})$ by integrating $\tilde{f}_X(x)$ in (67) over the region $[b_1^{(1)}, b_2^{(1)}] \times [b_1^{(2)}, b_2^{(2)}]$ and

compared the results with simulation. In Fig. 7.(b) we provided the $E_X^{(S,A)}(b^{(1)}, b^{(2)})$ for the same mobility parameter choices we considered in Fig. 7.(a). From the values of $E_X^{(S,A)}(b^{(1)}, b^{(2)})$ for different $[b_1^{(1)}, b_2^{(1)}] \times [b_1^{(2)}, b_2^{(2)}] \subseteq R$, we reached to the conclusion that the approximation we stated by (66) for the long-run spatial distribution of the random waypoint model over the given rectangular mobility terrain is quite accurate. Also notice that, the percentage of errors (i.e., $E_X^{(S,A)}(b^{(1)}, b^{(2)}) \times 100$) presented in Fig. 7.(a). are better than the ones in Fig. 7.(b). This is expected because to evaluate the $E_X^{(S,A)}(b^{(1)}, b^{(2)})$ in Fig. 7.(a), we computed $F_X(x, \Delta x_1, \Delta x_2)$ directly from equation (43). However, in Fig. 7.(b), we approximated $L(x_s, x_d, x, \Delta x_1, \Delta x_2)$ by equation (59) to evaluate $F_X(x, \Delta x_1, \Delta x_2)$, which decreased the quality of the approximation but gave us an approximation to $f_X(x)$ in closed form.

In addition, if one is interested in a variant of random waypoint mobility model where mobiles may pause at different X_d , that is, $f_{T_p|X_d}$ needs to be employed in mobility characterization instead of f_{T_p} , then the approximation given in (67) can be redefined as follows:

$$\tilde{f}_X(x) = \frac{E[T_p|X_d = x] \frac{1}{a_1 a_2} + E[\frac{1}{V}] k(x) / \tilde{N}}{E[T_p|X_d \in R] + E[\frac{1}{V}] \bar{D}} \quad (71)$$

where $E[T_p|X_d = x]$ is the expected pause time at the destination point x , and

$$E[T_p|X_d] = \int_{x_d \in R} dx_d f_{X_s}(x_d) E[T_p|X_d = x_d] \quad (72)$$

Finally, we note that in [5] authors also present a very accurate approximation for the pdf of X for the special case of the original random waypoint model where $R = [0, 1] \times [0, 1]$, and speed choice for all movement epochs is constant. In order to compare that approximation with the one given in this paper numerically for this special case (i.e., $R = [0, 1] \times [0, 1]$ and speed is constant), we evaluated cumulative long-run location distributions for several subregions over R according to both of them. We observed for various choices of $E[T_p]$ and V that the relative error between the results obtained from approximation and simulation is at most 2% for both of the approximation methods defined in [5] and in (66).

Example 2: According to the results that are proved in [1] for the one-dimensional version of the random waypoint mobility model, the probability distribution function of X_1 (i.e., the first component of $X = (X_1, X_2)$) over the mobility terrain $R = [0, a_1]$ is

$$F_{X_1}(x_1) = \frac{\frac{x_1}{a_1} E[T_p] + \frac{x_1^2(a_1 - 2x_1/3)}{a_1^2} E[\frac{1}{V}]}{E[T_p] + \frac{a_1}{3} E[\frac{1}{V}]} \quad (73)$$

Now, it is clear that an approximation to the marginal distribution of X_1 can be stated from the approximation defined by (66) for the joint probability density function of $X = (X_1, X_2)$ as follows:

$$F_{X_1}^{(A)}(x_1) = \int_0^{x_1} du \int_0^{a_2} dv \tilde{f}_X(u, v) \quad (74)$$

In principle, if \tilde{f}_X can closely approximate f_X , then the distribution $F_{X_1}^{(A)}(x_1)$ defined by (74) should also closely

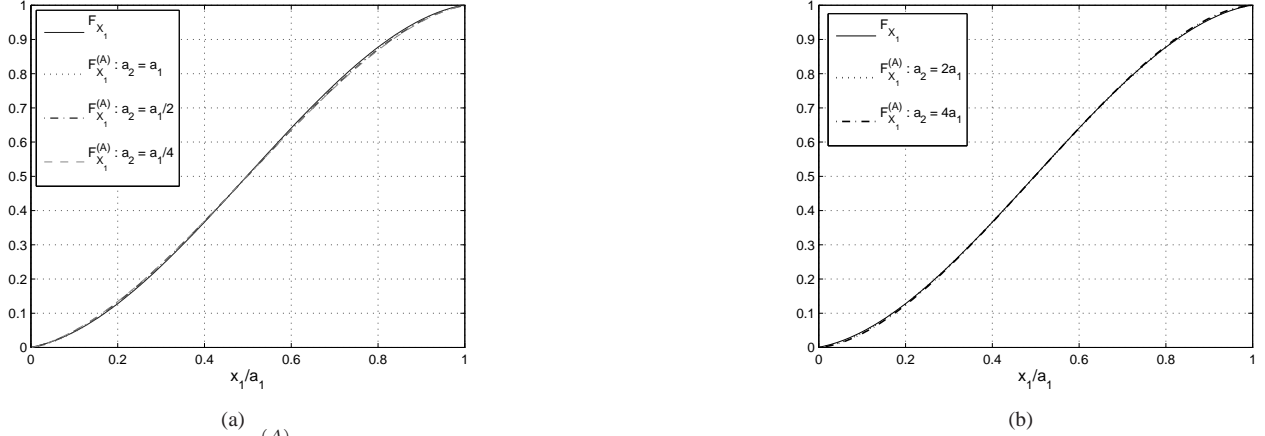


Fig. 8. Comparison of F_{X_1} and $F_{X_1}^{(A)}$ for Example 2 ($a_1 = 1000$ m, $\Delta x_1 = \Delta x_2 = 5$ m, $v_{min} = 1$ m/s, $v_{max} = 20$ m/s, $T_p = U[0, 30]$ sec).

approximate $F_{X_1}(x_1)$ in (73). To examine the correctness of this statement, in Fig. 8 we consider several proportions between a_1 and a_2 for the given mobility parameters, and provide a comparison of them. As it can be observed from Fig. 8, the two distribution functions perfectly matches with each other for several proportions between a_1 and a_2 . This observation is very important because it points out that the quality of approximation defined by $\tilde{f}_X(x)$ in (66) for $f_X(x)$ is insensitive to the frequency of the movement epochs that happen over the region $R = [0, a_1] \times [0, a_2]$ on the vertical and the horizontal directions. Hence, the approximation to $f_X(x)$ defined in equation (66) becomes applicable to any rectangular region.

Example 3: In Section IV, we stated that if the distribution of V (i.e., the speed for a movement epoch) is independent from X_s and X_d , then the pdf of \tilde{V} (i.e., $f_{\tilde{V}}$) and its expected value (i.e., $E[\tilde{V}]$) can be approximated by equations given in (51). As we have mentioned before, those equations are consistent with the ones given in [7] for a class of mobility models where V selected independently from the distance that is going to be traveled (i.e., $|X_s - X_d|$).

Thus, for this example, we consider a variant of random waypoint mobility model which incorporates the ability to determine V according to $|X_s - X_d|$, and concentrate on the accuracy of the approximation to the distribution of \tilde{V} we stated in Approximation 1 for the most generic mobility characterization.

Now for the original random waypoint model, keeping the distributions of X_d and T_p the same as before, consider a truncated normal distribution [17] for V according to the pdf given by

$$f_{V|X_s, X_d}(v|x_s, x_d) = \frac{Z\left(\frac{v - \mu(x_s, x_d)}{\sigma}\right)}{\sigma\left(\Phi\left(\frac{v_{max} - \mu(x_s, x_d)}{\sigma}\right) - \Phi\left(\frac{v_{min} - \mu(x_s, x_d)}{\sigma}\right)\right)} \quad (75)$$

for $v_{min} \leq v \leq v_{max}$ where $\sigma > 0$, and

$$\mu(x_s, x_d) = v_{min} + \frac{(v_{max} - v_{min})}{a} |x_s - x_d| \quad (76)$$

Z and Φ are the probability density and cumulative distribution functions for the normal distribution [17].

Before proceeding further, observe from the formulation of $f_{V|X_s, X_d}$ that as $\sigma \rightarrow 0$ the possibility of determining V proportional to $|X_s - X_d|$ increases. Also, as $\sigma \rightarrow \infty$ we converge to the original case, that is, V is uniformly distributed in $[v_{min}, v_{max}]$.

Now formulating the $f_{\tilde{V}}$ according to the equation (44) provided in Approximation 1, observe first that the integrand of $K(x, v, \Delta x_1, \Delta x_2)$ in (45) will be given by

$$k(x_s, x_d, x, v, \Delta x_1, \Delta x_2) = \frac{1}{(a_1 a_2)^2 v} f_{V|X_s, X_d}(v|x_s, x_d) L(x_s, x_d, x, \Delta x_1, \Delta x_2), \quad (77)$$

which implies that finding a closed form expression for $K(x, v, \Delta x_1, \Delta x_2)$ is very complicated even if the approximation defined by (59) for $L(x_s, x_d, x, \Delta x_1, \Delta x_2)$ is applied.

Therefore, to obtain an approximation to the distribution of \tilde{V} we use the numerical integration methodology we explained before in Example 1. Also, to test the accuracy of the numerical results obtained, we modified the simulation model we presented in Example 1 according to the new mechanism to select V , and finally obtained the probability distribution function of \tilde{V} , (i.e., $F_{\tilde{V}}(v) = \int_{v_{min}}^v du f_{\tilde{V}}(u)$) both from the $f_{\tilde{V}}$ given in Approximation 1 and the simulation model. In Fig. 9 we provide a comparison of these two results for different values of σ for the given mobility parameters. Simulation results are acquired with a 95% confidence interval lower than 0.003. Observe that, the two distributions perfectly matches with each other for all cases.

Having provided this confidence for approximation to the distribution of \tilde{V} defined by Approximation 1, we now focus on the effect of the choice of σ on the value of $E[\tilde{V}]$, which is also formulated by (50). In Table II, we provided $E[\tilde{V}]$ for different choices of σ and $E[T_p]$. The other parameters are the same with the experiments performed for the results depicted in Fig. 9. First, observe that for a given $E[T_p]$, $E[\tilde{V}]$ increases as σ decreases. Also, for a given finite value of σ , the difference between the $E[\tilde{V}]$ obtained, and the $E[\tilde{V}]$ evaluated for the $\sigma \rightarrow \infty$ case increases as $E[T_p]$ increases. Both of these results are expected because as σ decreases, the possibility of moving long distances with artificially low speeds diminishes, and as a result, the expected value of the long-run speed increases.

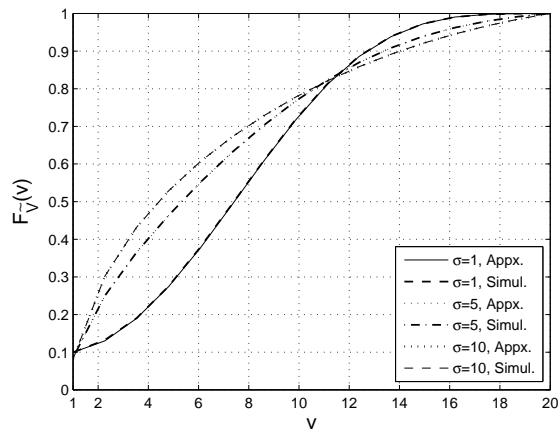


Fig. 9. Comparison of $F_{\hat{V}}$ derived from Approximation 1 and Simulation for Example 3 ($a_1 = 1200$ m, $a_2 = 900$ m, $\Delta x_1 = \Delta x_2 = 5$ m, $v_{\min} = 1$ m/s, $v_{\max} = 20$ m/s, $T_p = U[0, 30]$ sec).

TABLE II
 $E[\hat{V}]$ FOR EXAMPLE 3

$E[T_p]$ (sec)	$E[\hat{V}]$ (m/s)			
	$\sigma \rightarrow \infty$	$\sigma = 10$	$\sigma = 5$	$\sigma = 1$
0	6.342	6.517	6.867	8.106
15	5.408	5.985	6.279	7.299
30	4.713	5.535	5.785	6.638

VI. SUMMARY

This paper concentrates on the analysis of a generalized random mobility modeling approach for wireless ad hoc networks over two-dimensional mobility terrains. The analytical framework we introduced is based on a special discretization technique, and provided the long-run location and speed characteristics in full generality for a limited version of the model proposed where mobiles are only allowed to move towards one of the finite number of available directions. We provided approximations to the long-run distributions of the exact mobility formulation, where mobiles can move at any direction, from the analysis of this limited case. We also examined the accuracy and applicability of our approximations for a number of scenarios including random waypoint mobility model and a variant of it where the distribution of speed selected for a movement epoch is dependent on the distance that is going to be traveled.

From application of the results to random waypoint mobility model we derived an approximation to the long-run location distribution over rectangular mobility regions. We validated the accuracy of the approximation by simulation, and after comparing the marginals with proven results for one-dimensional regions pointed out that accuracy is insensitive to proportion between the dimensions of the rectangular region. Our analysis and example scenarios indicate that rich mobility models can be efficiently brought into the analytical studies concentrating performance characteristics of wireless ad hoc networks.

REFERENCES

[1] D. N. Alparslan and K. Sohraby, "A generalized random mobility model for wireless ad hoc networks and its analysis: One-dimensional case," University of Missouri- Kansas City, School of Computing

and Engineering, Tech. Rep., Dec. 2004. [Online]. Available: <http://www.sce.umkc.edu/~sohrabyk/>

[2] C. Bettstetter, "Smooth is better than sharp: a random mobility model for simulation of wireless networks," in *Proc. 4th ACM Int. Workshop on Modeling Analysis and Simulation of Wireless and Mobile Systems (MSWiM)*, Rome, Sept. 2001, pp. 19–27.

[3] T. Camp, J. Boleng, and V. Davies, "A survey of mobility models for ad hoc network research," *Wireless Communications & Mobile Computing (WCMC): Special issue on Mobile Ad Hoc Networking: Research, Trends and Applications*, vol. 2, no. 5, pp. 483–502, 2002.

[4] D. B. Johnson and D. A. Maltz, "Dynamic source routing in ad hoc wireless networks," in *Mobile Computing*, Imielinski and Korth, Eds. Dordrecht, The Netherlands: Kluwer Academic Publishers, 1996, vol. 353.

[5] C. Bettstetter, G. Resta, and P. Santi, "The node distribution of the random waypoint mobility model for wireless ad hoc networks," *IEEE Trans. Mobile Computing*, vol. 2, no. 3, pp. 257–269, 2003.

[6] W. Navidi and T. Camp, "Stationary distributions for the random waypoint mobility model," *IEEE Trans. Mobile Computing*, vol. 3, no. 1, pp. 99–108, 2004.

[7] J. Yoon, M. Liu, and B. Noble, "Sound mobility models," in *Proc. ACM MOBICOM*, San Diego, Sept. 2003, pp. 205–216.

[8] D. N. Alparslan and K. Sohraby, "Two-dimensional modeling and analysis of generalized random mobility models for wireless ad hoc networks," University of Missouri- Kansas City, School of Computing and Engineering, Tech. Rep., Mar. 2005. [Online]. Available: <http://www.sce.umkc.edu/~sohrabyk/>

[9] E. Çinlar, *Introduction to Stochastic Processes*. Prentice-Hall Inc., 1975, ch. 10.

[10] W. Feller, *An Introduction to Probability Theory and Its Applications*, 2nd ed. Wiley, 1970, vol. II, ch. 6.

[11] T. H. Cormen, C. E. Leiserson, and R. L. Rivest, *Introduction to Algorithms*. The MIS press, 1989, ch. 35.

[12] W. B. Davenport, *Probability and Random Processes*. McGraw-Hill, 1970, ch. 5.

[13] P. J. Davis and P. Rabinowitz, *Methods of Numerical Integration*, 2nd ed. Academic Press, 1983, ch. 1.5.

[14] M. Abramowitz and I. A. Segun, Eds., *Handbook of Mathematical Functions*. Dover Publications, 1970, ch. 25.

[15] D. M. Blough, G. Resta, and P. Santi, "A statistical analysis of the long-run node spatial distribution in mobile ad hoc networks," in *Proc. 5th ACM Int. Workshop on Modeling Analysis and Simulation of Wireless and Mobile Systems (MSWiM)*, Atlanta, Sept. 2002, pp. 30–37.

[16] C. Bettstetter and C. Wagner, "The spatial node distribution of the random waypoint mobility model for wireless ad hoc networks," in *Proc. First German Workshop Mobile Ad-Hoc Networks (WMAN)*, 2002, pp. 41–58.

[17] N. L. Johnson and S. Kotz, *Continuous Univariate Distributions-1*. Houghton Mifflin, 1970, vol. I, ch. 13.



Denizhan N. Alparslan received B.S. degree in mathematics from Middle East Technical University, Ankara, Turkey in 1998. He received the M.S. degree in computer engineering from Bilkent University, Ankara, Turkey in 2000, and Ph.D. degree in computer science from University of Missouri-Kansas City in 2005.

Since 2005, he has been with the Simulink V&V group, The MathWorks, Inc. His current research areas include network performance evaluation, queueing analysis, and model-based design.



Khosrow Sohraby (S'82-M'84-SM'89) received B.Eng and M.Eng degrees from McGill University, Montreal, Canada in 1979 and 1981, respectively, and Ph.D degree in 1985 from the University of Toronto, Toronto, Canada, all in Electrical Engineering.

His current research interests include design, analysis and control of High Speed computer and communications networks, traffic management and analysis, multimedia networks, networking aspects of wireless and mobile communications, analysis of algorithms, parallel processing and large-scale computations. Refer to www.sce.umkc.edu/~sohrabyk/ for detailed biography.